THE UNIVERSITY OF ALBERTA

POLARIZATION CHARACTERISTICS
OF
GEOMAGNETIC MICROPULSATIONS

BY

© RONALD DOUGLAS KURTZ

A THESIS

SUBMITTED TO THE FACULTY OF GRADUATE STUDIES

IN PARTIAL FULFILLMENT OF THE REQUIREMENTS

FOR THE DEGREE OF MASTER OF SCIENCE

DEPARTMENT OF PHYSICS

EDMONTON, ALBERTA

CANADA

FALL 1969

UNIVERSITY OF ALBERTA

FACULTY OF GRADUATE STUDIES

The undersigned certify that they have read, and recommend to the Faculty of Graduate Studies for acceptance a thesis entitled POLARIZATION CHARACTERISTICS OF GEOMAGNETIC MICROPULSATIONS, submitted by Ronald Douglas Kurtz, in partial fulfillment of the requirements for the degree of Master of Science.

ABSTRACT

Geomagnetic micropulsations were continuously recorded during the summer of 1968 at the University of Alberta Geophysical Observatory. Simultaneous measurements were made at a series of field locations in Alberta with truck mounted instrumentation. The analogue records were electronically converted to digital form and power spectral density estimates were obtained using Fast Fourier Transform techniques. From these spectral estimates the polarization characteristics were computed for the horizontal magnetic field variations having a period range from 10 to 273 seconds. The polarization characteristics are displayed as a function of period and time of day.

The averaged results indicate that the magnetic signal was polarized from north to N60°E. Micropulsations falling into the Pi2 class were found to be predominantly polarized in the counterclockwise sense, while Pi1's were polarized in the clockwise sense. Pc3's were polarized in the clockwise sense in the local morning and in the counterclockwise sense in the local afternoon while Pc4's were counterclockwise before local noon and clockwise in the afternoon.

ACKNOWLEDGEMENTS

I wish to express my sincere thanks to Dr. D. Rankin who made possible this research problem. His council and encouragement was indispensable throughout the entire programme.

I am grateful to Mr. M. D. Burke who designed and built the recording system and the digitizing system and for his assistance in preparing Chapter II.

I would also like to thank Dr. G. Rostoker for his advice and discussions which helped to forward the progress of this research.

I am indebted to Dr. W. J. Peeples for his advice and guidance at every critical period in this work, for aid in writing programmes, and for his careful reading of the manuscript of this thesis.

Mr. I. K. Reddy gave much assistance in analysing the data.

I am grateful to Mr. N. Ouellette who spent many long hours in collecting the field data and in digitizing the analogue records.

I would especially like to thank Miss D. Brown for her help in preparing the diagrams and for her

excellent job of typing this thesis.

During the course of this research the author was supported by the National Research Council of Canada.

TABLE OF CONTENTS

Page

CHAPTER 1 INTRODUCTION

CHAPTER 2 INSTRUMENTATION AND DATA PROCESSING

2.3 Spectral Analysis

LIST OF ILLUSTRATIONS

CHAPTER 1

INTRODUCTION

1.1 Definition of Micropulsations

For over a century it has been known that the Earth's geomagnetic field exhibits amplitude variations. These variations can range in period from small fractions of a second to many millions of years. It has been realized that much information concerning the Earth's interior and crust, ionosphere and magnetosphere can be obtained from studies made on these variations. In recent years interest has been shown in the magnetic field fluctuations known as geomagnetic micropulsations. This class includes all the fluctuations having a period falling in the range from about 0.2 seconds to 10 minutes. Their amplitudes can vary from the smallest detectable value (which is the order of a few milligammas at present) up to a few hundred gammas on rare occasions.

Studies of the characteristics of micropulsations have led to the separation of this activity into various groups. Many authors have devised their own classification systems, but a certain amount of difficulty is encountered due to uncertainties in the origin of micropulsations and their inter-relationships. To standardize the nomenclature

used, a classification system was approved at the thirteenth General Assembly of the IUGG in Berkeley, California (Jacobs et al., 1964).

In this classification, micropulsations were divided into two main classes: those of regular and continuous appearance called Pc, and those with an irregular form called Pi. The Pc group was further divided into five subgroups and the Pi group into two subgroups. These subgroups are shown in Table I.

TABLE I

CLASSIFICATION OF MICROPULSATIONS

CLASSIFICATION	PERIOD (SECONDS)	CLASSIFICATION	PERIOD (SECONDS)
Pc1	0.2-5.0	Pi1	1-40
Pc2	5.0-10.0	Pi2	40-150
Pc3	10-45		
Pc4	45-150		
Pc5	150-600		

A general picture of the pulsation spectrum is shown in Figure 1.1 (after Campbell, 1966).

Figure 1.1 General picture of the geomagnetic pulsation spectrum for the lower frequencies (Campbell, 1966).

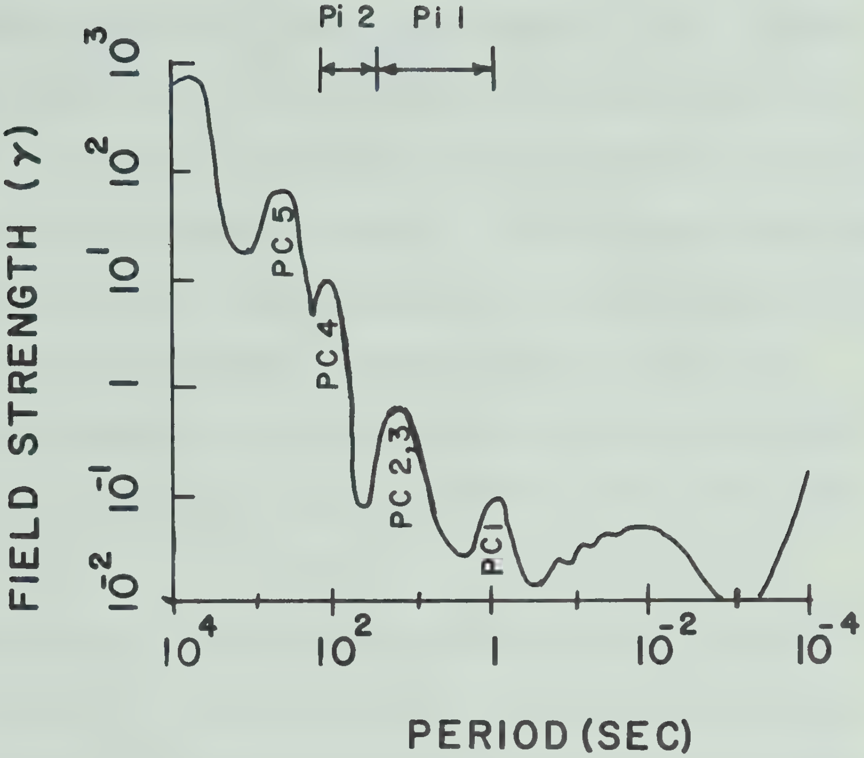

Pulsation	Period
Pc 1	0.2-5.0
Pc 2	5.0-10.0
Pc 3	10- 45
Pc 4	45-150
Pc 5	150-600
Pi 1	1 - 40
Pi 2	40-150

1.2 Literature Review

Numerous studies have been made to gain further insight into the source mechanisms of micropulsations. Considerable interest has been shown in recent years in their polarization characteristics. This thesis analyses these characteristics for micropulsations having a period range of 10 to 273 seconds. Since both Pi and Pc pulsations were analysed, it is necessary to determine how polarization characteristics vary between Pi1-2's and Pc3-5's.

Polarization studies have often been done by tracing out the tip of the magnetic perturbation vector in a plane, (the hodogram technique). If the variations of the magnetic field are polarized then, in general, an elliptical form will be traced out. Linear and circular forms occur only rarely.

Since polarization properties are heavily dependent on the time of day, latitude, and frequencies present in the micropulsation event, a brief review of observations on these factors is presented here. Since complete reviews are to be found elsewhere (Jacobs and Westphal (1964), Campbell (1967), and Saito (1969)), it was felt necessary to include here only observations on the

period and time of day occurrence of micropulsations.

1.2.1 Occurrence Frequencies and Period Content of Micropulsations

(a) Pi Micropulsations

Pi2 pulsations have been found to predominate in the nighttime and have a maximum occurrence frequency around local midnight, (Romañá and Cardús, 1962). However, they have also been detected in the daytime (Voelker, 1968). Pi1 pulsations often appear at the beginning of Pi2 events and also appear as riders on the longer period Pi2's. Jacobs and Sinno (1960a) have shown that their amplitude falls off to the north and south of the auroral zone. It has been found by Yanagihara (1959) that, as solar activity increases, Pi2 occurrence decreases, but it is just the opposite for Pi1 pulsations. However, the Pi2 occurrence frequency increases with increasing magnetic activity.

Pi2's can exhibit fairly complex frequency spectrums. Rostoker (1967a) found a linear relationship, in middle latitudes, between the number of frequency components in Pi2 events and Kp index. The number of

frequency components increases as the Kp index increases. On the average, he finds that the dominant periods lie between 100 seconds to 130 seconds. Rostoker also reports that these frequency components are not generally harmonics of a fundamental frequency so it is possible to consider that each frequency has its own separate generation mechanism. However, Hirasawa and Nagata (1966) at the Kakioka Field Station (ϕ = 36°14'N, λ = 140°11'E) found that in 58 samples of Pi2 pulsations, 74% consisted of a fundamental period and at least one harmonic component. Nwaigwe et al. (1967) analysed the pulsation activity recorded in south-west England in the period range from 10 seconds to 150 seconds. They reported an average period of about 80 seconds at night, but it varies from 110 seconds at 2230 GMT to about 40 seconds at 0400 GMT. Saito and Matsushita (1968) found the period of Pi2 to be between 60 to 90 seconds. They obtained this result by using digital dynamic spectrums of pulsations recorded at Fredericsburg (ϕ = 38°12'N, λ = 102°38'W).

(b) Pc Micropulsations

The Pc type pulsations have been found to be more prevalent in the daytime hours (Jacobs and Sinno, 1960b).

Pc2 and Pc3 pulsations usually have an amplitude of about 0.5 gamma. Campbell (1967) believes that the duration of these signals is related to the sensitivity of the recording device. They are always present but are at times too small to detect. Pc2 and Pc3 are reviewed together here as there seems to be no distinct spectrum separation between them. Hirasawa and Nagata (1966) report that Pc3 pulsations at the Kakioka Field Station appear only in the local daytime from 0600 hours to 2000 hours and are most active around local noon. Nwaigwe et al. (1967) found that during the morning hours, Pc3 activity had an average period of about 33 seconds and in the afternoon, an average period of about 40 seconds. This trend was also noted by Voelker (1968) in his studies of stations in Europe. Also Hirasawa and Nagata (1966) noted that the average period increased from 25 seconds at 0600 hours LT to 33 seconds at 1800 hours LT. These average periods are smaller than those found by Nwaigwe et al. (1967). This is perhaps explained by the fact that Voelker (1968) finds a systematic increase in the period of Pc2 and Pc3 in the daytime of the north-south component of the magnetic field with increasing latitude. Kato (1964), on the other hand, states that Pc3 pulsations have the longest period around noon and the shortest period around dawn. Entirely different results were found by

Christoffel and Linford (1966) in New Zealand. They found the average period to decrease from 40 seconds at 0400 hours LT to 27 seconds near local noon, and then increase again to 40 seconds at about 1800 hours LT. These results were obtained by visual analysis. Some of this confusion may arise due to the fact that Pc3 pulsations with a shorter period at noon (U-Type) tend to appear in the sunspot minimum years while those with longer periods around noon (inverted U-type) appear at the times of sunspot maximum. The average period of Pc3's has been found to increase with decreasing sunspot activity while Pc4 period decreases. Pc4 pulsations tend to be of the U-type and are active during sunspot minimum years. Therefore, Pc3's can be distinguished from Pc4's during sunspot maximum years, but during sunspot minimum years, Pc3's are masked by Pc4's intruding into them. The diurnal period variation observed will depend, then, on the year of the observation (Saito, 1969).

Pc4 micropulsations have an amplitude that ranges from 5 to 20 gammas, in the higher latitudes and an event can last from 10 minutes to several hours. They can also take a beating form, or have a damped appearance. Hirasawa and Nagata (1966) report that Pc4 pulsations are

continuous throughout the day, but are most active in the morning hours with the maximum occurring around 0800 hours LT. They found that the average period was 50 seconds around 0700 hours LT and 111 seconds around 1900 hours LT. Saito (1964) found an occurrence maximum at midday in middle and equatorial latitudes.

Pc5 pulsations have the largest amplitudes and are sometimes called Pg's or giant pulsations. They have quite a sinusoidal appearance and can be damped, but if the magnetic activity is high, some distortion can occur. Pc5's display a daytime occurrence pattern. Campbell (1967) states that near the northern auroral zone, Pc5 pulsations occur most frequently near 0600 hours and 1800 hours LT. However, at middle latitudes, a noon maximum is also reported. Herron (1967) averaged 80 records from the Lebanon State Forest, New Jersey, station to obtain the periods of spectral peaks. He found that the spectrum peaks at 227, 285 and 393 seconds. These spectral peaks had the highest amplitude on the days of high Kp index.

This, then, gives a general review of the characteristics of micropulsations. While many interesting facts have been obtained, much work still remains to be done. Many workers have analysed records that display

only simple, uncontaminated signal. They have avoided records that have several frequency components present and have irregular amplitudes. This is especially true on studies of polarization.

1.2.2 Polarization Characteristics of Micropulsations

Polarization characteristics have been determined mainly by visual inspection of magnetograms and by plotting the end point of the perturbation vector. However, Paulson, Egeland and Eleman (1964), and Paulson (1968) have reported work done by analytical techniques. A review is given here of the results found by various researchers.

(a) Sense of Polarization

Zybin (1967) reports that results obtained in the USSR showed that the sense of rotation of the polarization ellipse was 80 to 90% counterclockwise for all micropulsations in the period range from 30 seconds to 1200 seconds in the local morning hours in middle northern latitudes. In the evening hours, however, 60 to 70% of the micropulsations had a clockwise sense of rotation. He reports that separation of the two senses occurs one or two hours before local midday - midnight.

Zybin did not appear to make a distinction between Pi and Pc events. Rostoker (1967b), however, studied 20 separate Pi2 events recorded simultaneously on a station array extending from Victoria to Montreal, Canada. He found that Pi2's are polarized predominantly in the counterclockwise sense at middle latitudes in the northern hemisphere. He found that, even if the source of the Pi2 micropulsations lay in the center of his east-west station array, the sense of polarization almost always remained constant. Kato et al. (1956) found, however, that Pi2's were polarized in the counterclockwise sense after local midnight and in the clockwise sense before.

Christoffel and Linford (1966) report that in New Zealand 61% of the Pi2 events had a clockwise sense and 37% were linear. Here, one must take into account the predicted reverse sense of rotation between the two hemispheres.

It seems, then that the preferred sense of rotation for Pi2's is still somewhat confused. The average results of all the local nighttime records analysed in this thesis showed that Pi2's are predominantly polarized in the counterclockwise sense. The Pi1 band however shows

different results as will be discussed in Chapter III.

In New Zealand, Christoffel and Linford (1966) found that 56% of Pc3's analysed between 0700 to 1900 hours LT were polarized in the counterclockwise sense and 11% were clockwise; the rest were linear. They reported that nighttime Pc3 and Pc4 events were weak and not a sufficient amount of data was collected to give significant results. Campbell (1967) reported that Kawamura et al. (1961) found that only 5% of Pc2-3 events had a linear form, the rest were elliptical. These results were found in middle latitudes. About 75% of the ellipses had a ratio of minor to major axis of less than 0.5.

For Pc4's, Campbell (1967) states that the sense of polarization is predominantly counterclockwise in the northern hemisphere. Mather, Gauss et al. (1964) reported, however, that the sense of Pc4's was divided into clockwise during the day (0600-1800 hours LT) and counterclockwise at night (1800-0600 hours LT) in middle northern latitudes.

One hundred and ninety Pc5 events were recorded at Point Barrow (ϕ = 71°18'N, λ = 156°46'W),College (ϕ = 64° 52'W, λ = 147°50'W) and Sitka (ϕ = 57°04'N, λ = 135°20'W) by Kato and Utsumi (1964). The analyses indicated a

counterclockwise sense of rotation before local noon and a clockwise sense in the afternoon. In the middle latitudes, Sano (1963) and Saito (1964), report that Pc5 polarization seems to have four sectors in which the polarization changes alternately from clockwise to counterclockwise. The results obtained in this thesis suggest that events classified as Pc5's are polarized in the counterclockwise sense. The longest period sampled, however, was 273 seconds and these results are not really representative of the entire Pc5 band.

(b) Angle of Polarization

The angle of polarization is defined in this thesis as the angle that the major axis of polarization ellipse makes with geographic north. It is defined as positive if it is to the east of north, and negative if it is to the west. Very few conclusive results seem to have been found previously on this aspect of micropulsations. Zybin (1967) states that the angle depends mainly on the characteristics of each recording station and not on the type of micropulsation being received. He observes that stations near simple but large extended geological structures have the major axis of the polarization ellipse perpendicular to the

strike of the structure. Zybin made this statement with reference to hourly averaged results as individual measurements of the angle show a good deal of scatter. This scatter, then, reflects the variations in the micropulsations themselves, whereas mean values show the influence of geologic structure.

Table II, reproduced from Zybin (1967), shows the preferred angles of polarization at several stations.

TABLE II

PREFERRED POLARIZATION DIRECTIONS OBSERVED AT DIFFERENT STATIONS

STATION	AZIMUTH OF PREFERRED DIRECTION	RESEARCHERS
Aburatsubo	16°NW	Hatakeyama (1938)
Bermudas	13°NE	Santirocco and Parker (1963)
Borok	38°NW	Kalashnikov and Zybin (1960) Zybin (1966)
Göttingen	65°NW	Untiedt (1961)
Kiruna	58°NW	Paulson et al. (1965)
Lovozero	32°NE	Barsoukov and Zybin (1961)
Petropavlovsk	03°NW	Zybin (1966)
Victoria	32°NW	Duffus and Shand (1958)

Zybin found that those stations located near regional extended geoelectric structures and shorelines (Aburatsubo (Japan), Borok (ϕ = 58°02'N, λ = 38°58'E), Göttingen (ϕ = 51°32'N, λ = 9°58'E), Kiruna (ϕ = 67°50'N, λ = 20°25'E), and Lovozero (ϕ = 67°58'N, λ = 35°58'E)) have a preferred direction of polarization perpendicular to the strike. Island stations such as the Bermudas, Petropavlovsk (ϕ = 53°06'N, λ = 158°38'E), and Victoria (ϕ = 48°30'N, λ = 123°24'W) are much more difficult to interpret. Since the Rocky Mountain Range was within 200 miles of all the recording stations used in this thesis, comparisons were made between the angle of polarization and the strike of these mountains.

Zybin (1964) reported that, statistically, the major axis of the polarization ellipse rotates clockwise from the average prevailing direction before midnight and rotates counterclockwise in the hours after midnight for both Pi and Pc events. Around midnight, however, he found that the angles are close to their preferred direction. From studies of models, Zybin (1967) found that the diurnal variation of the angle is due to the change in the sense of polarization. Correlations were made in this thesis between these two polarization aspects.

Zybin (1964) also found that Pc's had an angle of polarization that rotates counterclockwise relative to the average prevailing direction, in the morning, while in the evening, it rotates clockwise. Campbell (1967) states that the polarization angle is zero (i.e. the major axis of the ellipse is north-south) for Pc2's and Pc3's. He feels, however, that this is somewhat dependent on the local time of day. Kato (1964) supports this and finds that the north-south component of the magnetic field disturbance vector predominates at low latitudes. This indicates nearly linear polarization, showing that the principal axis of polarization is in the north-south direction. The diurnal variation of the major axis in Japan was found to be to the NNW during the day and to the NNE at night, (Kato and Saito, 1959; Kawamura, Kurusu et al., 1961). Christoffel and Lindford (1966), on the other hand did not seem to find any dominant angle for Pc3's in New Zealand. For a given Pc3 event, the direction tended to remain fairly constant in the afternoon, but a gradual change began near sunset.

According to Campbell (1967), Pc5 pulsations are usually elliptically polarized. The angle of polarization usually changes between the morning and evening peaks of

the diurnal frequency pattern (Kato, 1964).

1.3 Purpose of the Research

Many theoretical attempts have been made to explain the origin of micropulsations and consequently, have predicted a variety of polarization characteristics. The results presented in the previous section indicate that an entirely coherent experimental discription of the polarization characteristics has yet to be determined. A large amount of statistical information about geomagnetic micropulsations must be accumulated.

Until the last few years, polarization information was obtained by utilizing the hodogram technique. This technique requires that the signal be nearly periodic. Any contamination due to random noise or the superposition of several signals at different periods will result in an extremely confused hodogram. This was clearly demonstrated by Paulson (1968). Thus, detailed polarization studies of complicated magnetic field variations have not, in general, been attempted.

It is the purpose of this thesis to present the results using power spectral analysis and the techniques

outlined by Fowler et al. (1967) to analyse complicated magnetic signals. This technique was applied, for the first time, to a large number of records to determine statistically the hourly averaged values of the polarization characteristics as a function of period and time of day. Thus polarization characteristics of the geomagnetic micropulsation spectrum are clearly displayed for interpretation purposes.

CHAPTER 2

INSTRUMENTATION AND DATA PROCESSING

2.1 Signal Detection

Variations in the surface magnetic and electric fields were recorded using the instrumentation as described below. The surface variations have been analysed to determine the local resistivity structure of the earth. In this thesis the polarization characteristics of the magnetic field variations will be analysed.

Three mutually orthogonal induction coils were buried in the ground to measure the vertical (Hz), the geographic north-south (Hx) and the geographic east-west (Hy) components of the magnetic field variations. The coils consist of 32,000 turns of #28GA enamelled copper wire on a 60 inch x 0.75 inch high permeability core. The total resistance of the coil is 845 ohms and the total inductance is 850 henrys at 0.1 Hz.

The signal from the coils was fed into a pre-amplifier/post-amplifier system. The post-amplifier has gain settings from -20db to +20db in steps of 10db to permit the recording of various levels of signal strength. The signal was recorded on magnetic tape using a seven channel Precision Instrument analogue FM tape recorder with

a tape speed of 15/16 inches per second.

Six channels of data were recorded on the tape. Three channels record the mutually orthogonal magnetic field variations, two channels record the telluric field variations, and one channel records a WWVB time signal. The six signals were simultaneously recorded on a six channel Brush paper recorder for visual editing prior to the digitization process. A block diagram of the recording system is shown in Figure 2.1 and the frequency response of the magnetic system is shown in Figure 2.2.

2.2 Analogue to Digital Conversion

The Brush paper records were examined to insure that they contained sufficiently large amplitude signals, no discontinuities, and did not exceed the dynamic range of the recording apparatus (saturation). Suitable records, 3.6 hours long, were digitized with a digitizing interval of 32/15 seconds and a consequent Nyquist frequency of 0.234 Hz. A block diagram of the analogue to digital conversion system is shown in Figure 2.3. The analogue signal was passed through a low pass filter with a corner at 0.125 Hz and aliasing of the signal was thereby eliminated.

Figure 2.1 Block diagram of the recording system.

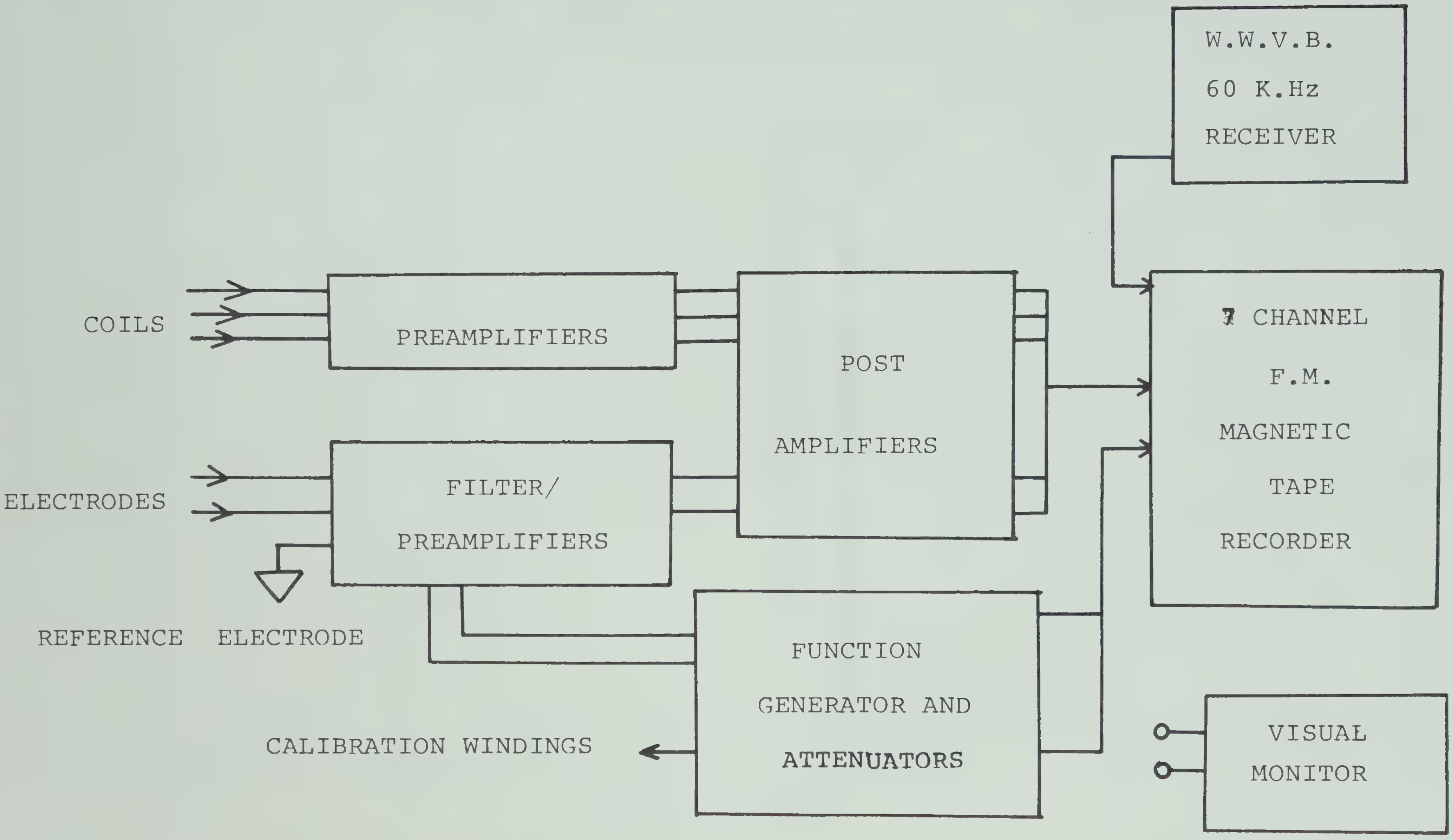
W.W.V.B.
60 K.Hz
RECEIVER
7 CHANNEL
F.M.
MAGNETIC
TAPE
RECORDER
COILS
PREAMPLIFIERS
POST
AMPLIFIERS
ELECTRODES
FILTER/
PREAMPLIFIERS
REFERENCE ELECTRODE
FUNCTION
GENERATOR AND
ATTENUATORS
CALIBRATION WINDINGS
VISUAL
MONITOR

Figure 2.2 Calibrated frequency response curve for the magnetic recording system.

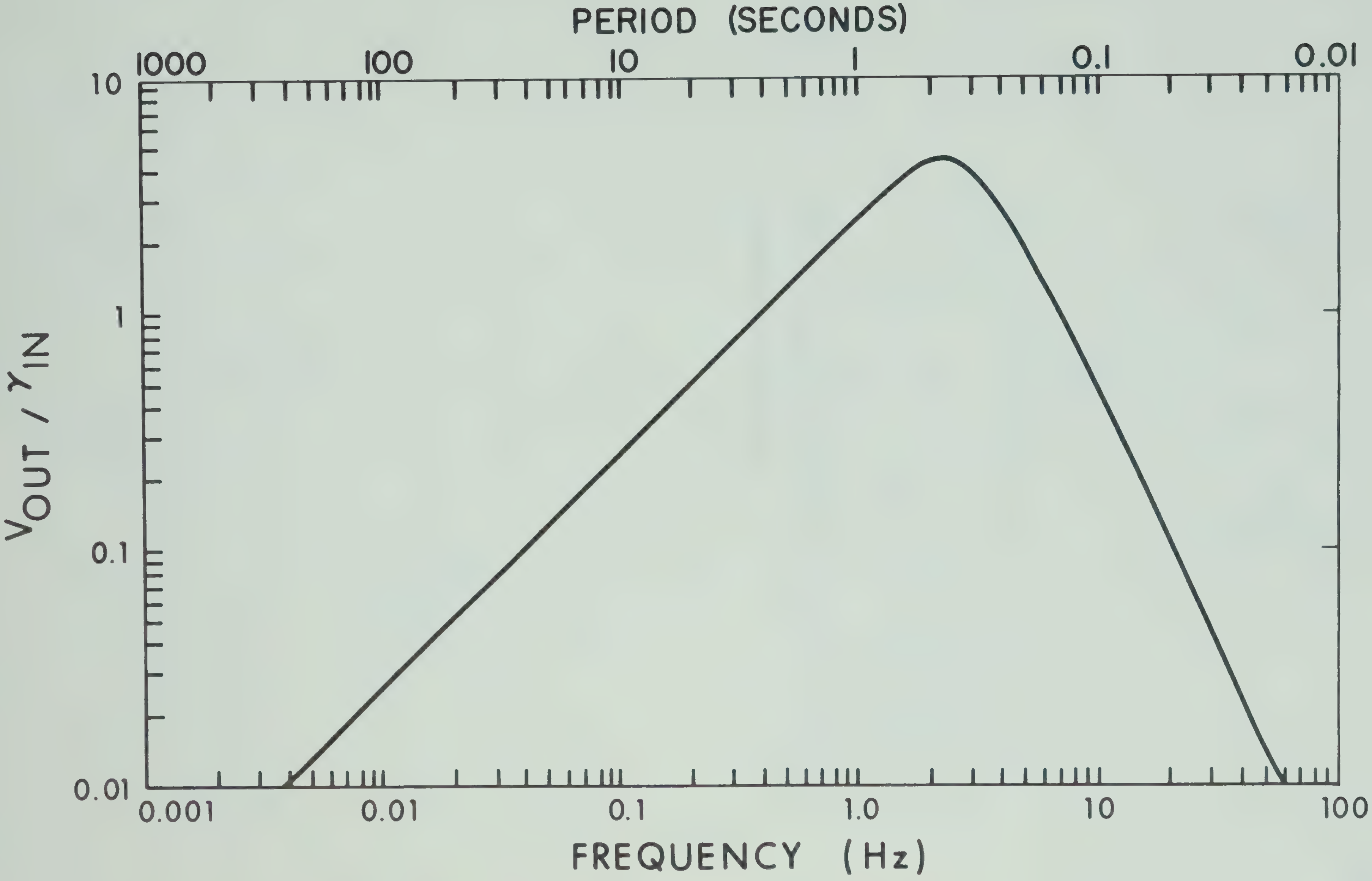
PERIOD (SECONDS)
1000
100
10
1
0.1
0.01
10
1
0.1
0.01
V_{OUT} / γ_{IN}
0.001
0.01
0.1
1.0
10
100
FREQUENCY (Hz)

Figure 2.3 Block diagram of the analogue to digital conversion system.

Digitized data were recorded on two, seven channel, asynchronous, incremental, Kennedy digital tape recorders. Each data point was stored in a 12 bit binary form with the least significant bit utilized for channel identification. Data blocks of 3600 two-character words were recorded alternately on the two Kennedy recorders to provide the Inter-Record-Gap required for input to the IBM 360/67 digital computer. The data were read from the two seven track tapes and stored on an IBM nine track tape for analysis purposes.

2.3 Spectral Analysis

The autopower and crosspower spectral estimates were calculated in order to use the method outlined (see section 2.4) for determining the polarization characteristics. A summary of the technique used for obtaining the autopower and crosspower spectral estimates will now be given.

2.3.1 Removal of Mean and Trend

The spectral analysis technique requires that the time series originates from a stochastic process with zero mean value. If the mean is not zero, the power spectrum

will have a large DC estimate which distorts estimates at other frequencies. If the record consists of N data points, u_n, where n = 1,2,....,N, the estimate of the mean is given by

$$\bar{u} = \frac{1}{N} \sum_{n=1}^{N} u_n \tag{2.1}$$

This mean value was removed from the time series.

Next, the method of Bendat and Piersol (1966) was employed to remove any slowly varying linear trends which can cause distortion of estimates. These trends could arise from instrument drift or actual trends. The average slope of the time series u(t) can be defined to be,

$$\bar{\alpha}_u = \frac{1}{(T/3)(2T/3)} \left[\int_{2T/3}^{T} u(t)dt - \int_{o}^{T/3} u(t)dt\right] \tag{2.2}$$

where T is the total record length. Rewriting equation 2.2 in a form suitable for digitized data gives

$$\bar{\alpha}_u = \frac{1}{\Delta\nu(N-\nu)} \left[\sum_{n=N-\nu}^{N} u_n - \sum_{n=1}^{\nu} u_n\right] \tag{2.3}$$

where Δ is the digitization interval and ν is the largest integer less than or equal to N/3. The data with zero mean value and zero average slope is then given

by

$$X_n = u_n - \overline{u} - \alpha_u(n\Delta - T/2)$$

$$n = 1,2,\ldots,N. \qquad (2.4)$$

It is important to note that prewhitening the time series was not considered necessary since the micropulsation power spectrum exhibits a natural 1/f dependence (where f denotes frequency), which is counteracted by the output of the induction coils which is proportional to the frequency. Hence, the coils effectively prewhiten the signal spectrum.

2.3.2 Calculation of the Autopower and Crosspower Spectral Estimates

The autopower and crosspower spectral estimates were calculated using the method of Blackman and Tukey (1958) combined with the Fast Fourier Transform (FFT) algorithm of Cooley and Tukey (1965) as applied by Gentleman and Sande (1966).

The FFT technique assumes that the data is cyclic; therefore, to avoid problems in the frequency domain, it is desirable that the initial and final data points of a time

series are smoothly continuous. To effect this, a cosine taper was applied to the initial and final 10% of the N data points.

Zeroes must be added to the time series to prevent the introduced cyclic structure of the data from distorting the autocovariance and crosscovariance estimates. The minimum number of zeroes required equals the maximum lag number to be calculated. The FFT programs available require that the total number of points, N', being analysed must be factorable in the radix of 2. Therefore, the final series of N' points is given by

$$N' = N + \text{number of zeroes} \qquad (2.5)$$

The discrete Fourier transform of the time series x_n is given by

$$X(W) = \frac{1}{N'} \sum_{n=0}^{N'-1} x_n e^{-2\pi i (\frac{W}{N}) j\Delta}$$

$$W = 0,1,2,\ldots.,N-1 \qquad (2.6)$$

where W is the digital frequency index. The angular frequency, ω, is related to W by

$$\omega = \frac{2\pi W}{N\Delta} .$$

Similarly, a second time series, y_n, will have a discrete

Fourier transform given by Y(W). The raw, unsmoothed crosspower estimate, Pxy(W), is then given by

$$Pxy(W) = X^*(W) \cdot Y(W) \qquad (2.7)$$

The asterisk denotes the complex conjugate. The Wiener-Khintchine theorem states that the crosscovariance and the crosspower spectrums are a Fourier transform pair. Therefore, the crosscovariance function, Cxy(τ), is given by

$$Cxy(\tau) = \frac{1}{N}\left[\sum_{W=0}^{N-1} \{X^*(W) \cdot Y(W)\}\, e^{+\frac{2\pi i W\tau}{N}}\right] \qquad (2.8)$$

This indirect method of calculating the crosscovariance requires much less computer time than the direct calculation of Cxy(τ).

The Parzen window (Parzen, 1961) was used to smooth the raw autocovariance estimates. This window requires a negligible amount of computation time and gives positive definite spectral estimates with extremely low side-lobes. The Parzen lag function is given by

$$\begin{aligned} R(\tau) &= 1-6\left(\frac{\tau}{m}\right)^2 + 6\left(\frac{\tau}{m}\right)^3 & |\tau| < \frac{m}{2} \\ &= 2\left[1 - \left(\frac{\tau}{m}\right)\right]^3 & \frac{m}{2} \leq |\tau| \leq m \qquad (2.9) \\ &= 0 & |\tau| > m \end{aligned}$$

where m is the maximum lag.

The smoothed crosspower estimates were then evaluated by the following computation:

$$Pxy(W) = \sum_{\tau=0}^{m-1} Cxy(\tau)R(\tau)e^{-\frac{2\pi iW\tau}{m}} . \qquad (2.10)$$

The smoothed autopower spectral estimates were obtained in a similar fashion by substituting

$$y_n = x_n \qquad n = 1,2,\ldots.,N$$

in equation 2.7.

2.3.3 Removal of the Digitizing Phase Shift

As mentioned in section 2.2, six channels of data were sampled sequentially to give a digitizing interval of 32/15 seconds. Thus, the digitized points on two adjacent channels had a real time separation of 32/90 second. This introduced a frequency dependent phase shift in the crosspower estimates.

To calculate the actual value of the phase shift, consider the Fourier transform of a function of time, x(t), with a time translation of α.

$$\begin{aligned} X(\omega) &= \int_{-\infty}^{\infty} x(t+\alpha)\, e^{-i\omega t} dt \\ &= e^{i\omega\alpha} \int_{-\infty}^{\infty} x(t) e^{-i\omega t} dt \\ &= e^{i\omega\alpha} \hat{X}(\omega). \end{aligned} \tag{2.11}$$

Similarly, a second function, y(t), with a time translation of β, has the following Fourier transform:

$$\begin{aligned} Y(\omega) &= \int_{-\infty}^{\infty} y(t+\beta) e^{-i\omega t} dt \\ &= e^{i\omega\beta} \hat{Y}(\omega). \end{aligned} \tag{2.12}$$

The crosspower is given by

$$Pxy(\omega) = X^*(\omega) \cdot Y(\omega) = \hat{X}^*(\omega) \cdot \hat{Y}(\omega) e^{i\omega(\beta-\alpha)} \tag{2.13}$$

If x(t) and y(t) are digitized and if x(t) is sampled first, then α is zero and β represents the relative time difference between the two sampled channels. The crosspower spectral estimates obtained by the analysis of the horizontal orthogonal magnetic components were multiplied by $e^{-i\omega\beta}$ to obtain the correct crosspower phase estimates.

Finally, it should be noted that induction coils measure the time derivative of the magnetic flux $\phi(t)$. The following property of the Fourier transform allows power estimates of the horizontal orthogonal magnetic intensity

components, Hx and Hy to be found:

$$\int_{-\infty}^{\infty} \frac{\partial\phi(t)}{\partial t} e^{-i\omega t}dt = i\omega \int_{\infty}^{\infty} \phi(t)e^{-i\omega t}dt \qquad (2.14)$$
$$= i\omega\, \hat{\phi}(\omega).$$

For a coil, the flux is linearly related to the magnetic intensity. Therefore, when the calibrated instrument response was removed in this analysis, power estimates in units of γ^2/cps were obtained.

2.4 Determination of Polarization Characteristics

The autopower and crosspower spectral estimates were used to calculate time varying polarization characteristics of geomagnetic micropulsations in different frequency bands by following the treatment outlined by Fowler et al. (1967).

Throughout the following, it is assumed that the vector disturbance recorded at a fixed point in space is quasi-monochromatic at the mean signal frequency, $\overline{f}$, of interest. Quasi-monochromatic means that if the frequency spectrum of a signal has a frequency peak of bandwidth Δf centered at frequency $\overline{f}$, then

$$\Delta f/\overline{f} < < 1. \qquad (2.15)$$

If Pxx(ω) and Pyy(ω) represent the autopower estimates of the north-south and east-west components respectively of the horizontal magnetic field intensity, and Pxy(ω) represents the crosspower estimates at angular frequency, ω then a coherency matrix can be defined as

$$J(\omega) = \begin{bmatrix} Pxx(\omega) & Pxy(\omega) \\ Pyx(\omega) & Pyy(\omega) \end{bmatrix}. \qquad (2.16)$$

The matrix is Hermitian since $Pxy(\omega) = P\overset{*}{y}x(\omega)$. The matrix may be expressed as the sum of a coherency matrix, L(ω), for the polarized portion of the signal and a coherency matrix U(ω) for the unpolarized portion:

$$J(\omega) = L(\omega) + U(\omega). \qquad (2.17)$$

The polarized portion may be written as

$$L(\omega) = \begin{bmatrix} C(\omega) & D(\omega) \\ D^{*}(\omega) & E(\omega) \end{bmatrix}, \qquad (2.18)$$

and the unpolarized portion as

$$U(\omega) = \begin{bmatrix} F(\omega) & G(\omega) \\ G^{*}(\omega) & I(\omega) \end{bmatrix}. \qquad (2.19)$$

For completely unpolarized signal, the mutual coherency must be zero:

$$\frac{|G(\omega)|}{[F(\omega) \cdot I(\omega)]^{\frac{1}{2}}} = 0. \qquad (2.20)$$

Since the matrix is Hermitian:

$$G(\omega) = G^{*}(\omega) = 0.$$

If one component were larger than the other, some degree of linear polarization would exist. Thus for the unpolarized contributions:

$$F(\omega) = I(\omega).$$

The coherency matrix for the unpolarized portion of the signal can be rewritten:

$$U(\omega) = \begin{bmatrix} F(\omega) & 0 \\ 0 & F(\omega) \end{bmatrix}. \qquad (2.21)$$

Equation 2.16 can now be written as

$$\begin{bmatrix} Pxx(\omega) & Pxy(\omega) \\ Pyx(\omega) & Pyy(\omega) \end{bmatrix} = \begin{bmatrix} C(\omega) & D(\omega) \\ D^{*}(\omega) & E(\omega) \end{bmatrix} + \begin{bmatrix} F(\omega) & 0 \\ 0 & F(\omega) \end{bmatrix}. \qquad (2.22)$$

As shown in Born and Wolf (1959), the determinant of the coherency matrix for a completely polarized signal is always zero. This fact enables the value of F(ω) to be determined. Rewriting equation 2.22 yields

$$\begin{bmatrix} C(\omega) & D(\omega) \\ D^{*}(\omega) & E(\omega) \end{bmatrix} = \begin{bmatrix} Pxx(\omega) - F(\omega) & Pxy(\omega) \\ Pyx(\omega) & Pyy(\omega) - F(\omega) \end{bmatrix}. \qquad (2.23)$$

Taking the determinant of both sides gives

$$F^2(\omega) - F(\omega)[Pxx(\omega) + Pyy(\omega)] + |J(\omega)| = 0,$$

where the vertical bars represent the value of the determinant. Therefore, the value of F(ω) is given as

$$F(\omega) = \tfrac{1}{2}[Pxx(\omega) + Pyy(\omega)] \pm \tfrac{1}{2}[(Pxx(\omega) + Pyy(\omega))^2 - 4|J(\omega)|]^{\frac{1}{2}}. \tag{2.24}$$

The root with the positive sign is rejected since it gives negative values for the autopowers of the polarized signal, C(ω) and E(ω), in equation 2.23.

The values of C(ω), E(ω), D(ω) and F(ω) can now be determined in terms of the original coherency matrix (equation 2.16).

$$\begin{aligned} C(\omega) &= Pxx(\omega) - F(\omega) \\ D(\omega) &= Pxy(\omega) \\ D^*(\omega) &= Pyx(\omega) \\ E(\omega) &= Pyy(\omega) - F(\omega). \end{aligned} \tag{2.25}$$

Thus, the intensity of the polarized portion of the signal is given by the trace of L(ω):

$$\begin{aligned} Tr[L(\omega)] &= C(\omega) + E(\omega) \\ &= [(Pxx(\omega) + Pyy(\omega))^2 - 4|J(\omega)|]^{\frac{1}{2}}. \end{aligned}$$

Then the degree of polarization which is the ratio of the polarized intensity to the total intensity is given by

$$R(\omega) = [1 - \frac{4|J(\omega)|}{(Pxx(\omega) + Pyy(\omega))^2}]^{\frac{1}{2}}. \qquad (2.26)$$

By using the coherency matrix for the polarized signal, $L(\omega)$, the polarization ellipse may be determined from

$$[y \ \ x] \begin{bmatrix} C(\omega) & D(\omega) \\ D^*(\omega) & E(\omega) \end{bmatrix} \begin{bmatrix} y \\ x \end{bmatrix} = C(\omega) \cdot E(\omega). \qquad (2.27)$$

Expanding equation 2.27 gives

$$\frac{x^2}{C(\omega)} + \frac{2ReD(\omega)}{C(\omega)\ E(\omega)} + \frac{y^2}{E(\omega)} = 1. \qquad (2.28)$$

Equation 2.28 is the equation of an ellipse in the coordinate system (x,y). The angle, $\theta(\omega)$, through which the coordinate axes must be rotated to align with the major and minor axes of the ellipse is called the angle of polarization. This is easily shown to be

$$\tan\ 2\theta(\omega) = \frac{2ReD(\omega)}{C(\omega)-E(\omega)}. \qquad (2.29)$$

Substitution of the values from equations (2.25) allows calculation of θ from spectral estimates. This gives

$$\tan 2\theta(\omega) = \frac{2\mathrm{Re}Pxy(\omega)}{Pxx(\omega)-Pyy(\omega)} .$$

If $\theta(\omega)$ is positive, the angle is measured clockwise from north.

The ratio of minor to major axis of the ellipse gives the ellipticity. The ellipticity is defined in terms of the angle $\theta(\omega)$ where

$$\sin 2\beta(\omega) = \frac{i(D^*(\omega)-D(\omega))}{[(C(\omega)-E(\omega))^2 + 4D^*(\omega)\cdot D(\omega)]^{\frac{1}{2}}}$$

where $i = \sqrt{-1}$.

Substitution of the values from equation (2.25) yields

$$\sin 2\beta(\omega) = \frac{i[Pyx(\omega)-Pxy(\omega)]}{[(Pxx(\omega)-Pyy(\omega))^2 + 4Pyx(\omega)Pxy(\omega)]^{\frac{1}{2}}} .$$

The ellipticity itself is given by $\tan \beta(\omega)$ which ranges from 1 for circularly polarized signal, to 0 for linearly polarized signal. If $\beta(\omega)$ is positive, the sense of polarization is counterclockwise when looking into the progating wave; the sense is clockwise if β is negative.

2.5 Implementation

The Hx and Hy autopowers, the angle, the degree,

and the sense of polarization, and the ellipticity were plotted as functions of period and of local time. The 3.6 hours record was divided into sections of 818 seconds. Each section overlapped the previous section by 382 seconds. Overlapping sections gave smoother changes in the autopowers and polarization parameters as they were plotted as functions of time for a particular period. Results were printed by the computer with local time as the abscissa and period as the ordinate. All the autopowers and polarization parameters were divided into intervals and assigned a value. This permitted contouring constant values of autopowers and polarization parameters as functions of local time and period.

Examination of the computer printout plots of angle, ellipticity and sense revealed small isolated "pockets" of confused results. These tended to occur when the degree of polarization was small. To facilitate contouring, the values for angle, ellipticity and sense were left blank on the plots when the degree of polarization was less than 50%. Since the signal was predominantly greater than 50% polarized, this resulted in only isolated pockets of blanks. When contouring was being done, these blank pockets were ignored for ease of interpretation.

CHAPTER III

THE RESULTS OF ANALYSIS OF MICROPULSATION DATA

3.1 Recording Stations

During the summer of 1968 measurements of the surface magnetic field variations were made at the University of Alberta Geophysical Observatory* near Leduc, Alberta ($\phi = 53°13'N$, $\lambda = 113°21'W$). Continuous recording was carried out between May 20 to June 20, 1968, and between August 1 to September 13, 1968. No recordings were taken between 0900 to 1000 hours LT** and between 2100 hours to 2200 hours LT** as this was the time that tapes were being changed on the recorders and calibrations of the instruments were being made. Records that contained no activity or that had exceeded the dynamic range of the tape recorders were discarded.

Rankin and Reddy (1969) have stated that anisotropic electrical conductivities exist in the Precambrian basement in the vicinity of the Observatory. It

---

* For brevity, the University of Alberta Geophysical Observatory will be called the Observatory in the remainder of this thesis.

** Local Time (LT) is Mountain Standard Time which is seven hours earlier than Universal Time.

was felt necessary, therefore, to compare the polarization parameters obtained at the Observatory to those made simultaneously at other sites. Thirteen field locations were chosen in central western Alberta and in southern Alberta. Their locations are shown in Figure 3.1. Also, their geographic coördinates are given in Table III. The dates and beginning times of the records analysed are given in Table IV. The records last 3.6 hours. Similar equipment as that used at the Observatory was mounted in a truck to record at the field sites. When two or three suitable eleven hour records had been recorded, the truck was moved to the next site.

Locations were chosen on the basis of isolation from human noise contamination. Thus sites were as far as possible from busy highways, electrical sources, construction and oil wells. Also the surface relief was small for at least several miles in all directions from the recording station. These conditions were easily met on the Prairies of southern Alberta. However, the stations of Nordegg, Foothills and Gregg Lake were located in the foothills of the Rocky Mountain Range and the surrounding relief was considerable at distances greater than half a mile from the site.

Figure 3.1 Map of Alberta showing the location of the recording stations.

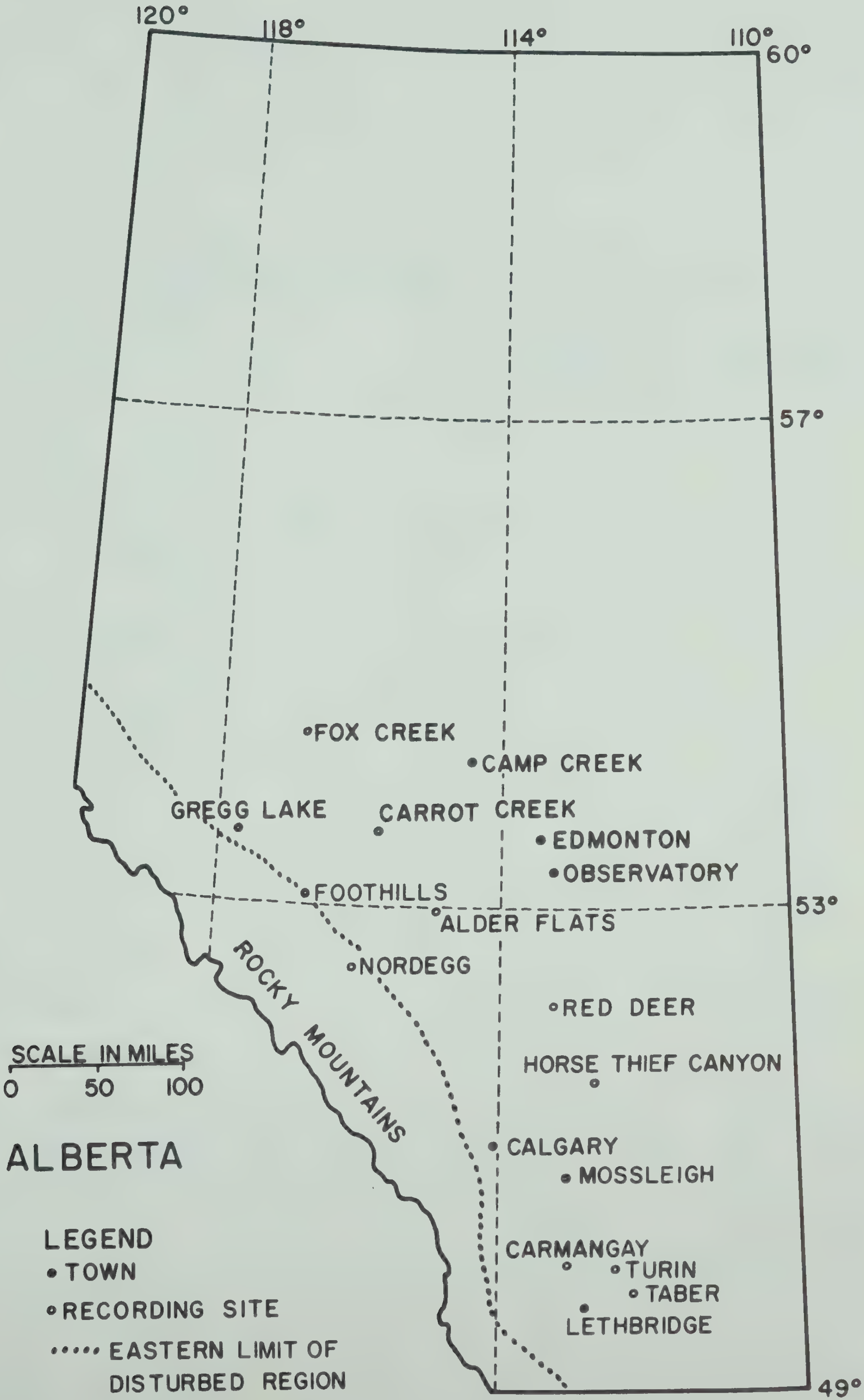
120°
118°
114°
110°
60°
57°
53°
49°
FOX CREEK
CAMP CREEK
GREGG LAKE
CARROT CREEK
EDMONTON
OBSERVATORY
FOOTHILLS
ALDER FLATS
NORDEGG
RED DEER
HORSE THIEF CANYON
CALGARY
MOSSLEIGH
CARMANGAY
TURIN
TABER
LETHBRIDGE
ROCKY MOUNTAINS
SCALE IN MILES
0
50
100
ALBERTA
LEGEND
• TOWN
∘ RECORDING SITE
••••• EASTERN LIMIT OF DISTURBED REGION

TABLE III

GEOGRAPHIC COORDINATES OF RECORDING SITES

STATION LOCATION	GEOGRAPHIC LATITUDE	GEOGRAPHIC LONGITUDE
Alder Flats	52°57'N	114°57'W
Camp Creek	54°13'N	114°32'W
Carmangay	50°5'N	113°18'W
Carrot Creek	53°36'N	115°52'W
Foothills	53°04'N	116°48'W
Fox Creek	54°26'N	116°55'W
Gregg Lake	53°30'N	117°50'W
Mossleigh	50°48'N	113°18'W
Horse Thief Canyon	51°34'N	112°55'W
Nordegg	52°28'N	116°05'W
Red Deer	52°10'N	113°27'W
Taber	49°51'N	112°17'W
Turin	50°2'N	112°31'W
University of Alberta Geophysical Observatory	53°13'N	113°21'W

TABLE IV

DATES, TIMES AND Kp INDICES FOR RECORDS ANALYZED

Station Location	Date	Starting Time of Field Records (LT)	Starting Time of Observatory Records (LT)	Kp Index for Field Records	Kp Index for Observatory Records
Alder Flats	Sept. 12/68	0354	0408	3- 4-	3- 4-
	Sept. 12/68	1143	1000	3+ 4-	4_o 3+
	Sept. 12/68		1334		3+ 4-
	Sept. 12/68	1719	1707	5+ 6-	5+ 6-
Camp Creek	Sept. 4/68	0103	0103	3- 4-	3- 4-
	Sept. 4/68	0425	0354	4- 3+	4- 3+
Carmangay	June 11/68	2221	2250	2-	2-
	June 12/68	0154		4_o	
Carrot Creek	Aug. 16/68	2253	2134	5-	5+ 5-
	Aug. 17/68	0159	0117	4+	4+ 4+
	Aug. 17/68	0505	0450	4_o	4_o
	Aug. 17/68	1005	0957	6- 3+	6- 3+
	Aug. 17/68	1615	1331	3_o	3+ 4-
	Aug. 17/68	1813	1704	3_o 4_o	3
Foothills	Aug. 14/68		2202		4_o 4_o
	Aug. 15/68	0302	0136	4+ 4_o	4+
	Aug. 15/68		0508		4_o

.continued.

TABLE IV Continued

DATES, TIMES, AND Kp INDICES FOR RECORDS ANALYZED

Station Location	Date	Starting Time of Field Records	Starting Time of Observatory Records	Kp Index for Field Records	Kp Index for Observatory Records
Fox Creek	Aug. 18/68	0000	2201	3_o 3_o	3- 3_o
	Aug. 19/68	0324	0134	3_o 2+	3_o
	Aug. 19/68	0553	0508	2+ 2_o	2+
Gregg Lake	Aug. 13/68	0943	0958	2+ 5-	2+ 5-
	Aug. 13/68	1412	1315	4-	5- 4-
	Aug. 13/68	1603	1704	4- 5-	5-
	Aug. 13/68	2200	2213	3_o	3_o 4_o
	Aug. 14/68	0213	0146	4_o	4_o
	Aug. 14/68	0530	0518	5- 3+	5-
Horse Thief Canyon	May 29/68	2351	2356	2+ 2_o	2+ 2_o
	June 1/68	1140	1057	4- 4-	3_o 4-
	June 1/68	2202	2154	2+ 2+	2+ 2+
Mossleigh	June 6/68	2251	2247	3- 4-	3- 4-
	June 7/68	0226	0222	3+ 3-	3+ 3-
	June 7/68	1007	1014	2- 1-	2- 1-
	June 7/68	1342	1349	1-	1-
	June 8/68	0446	0511	1- 1_o	1- 1_o

TABLE IV Continued

DATES, TIMES AND Kp INDICES FOR RECORDS ANALYZED

Station Location	Date	Starting Time of Field Records (LT)	Starting Time of Observatory Records (LT)	Kp Index for Field Records	Kp Index for Observatory Records
Nordegg	Aug. 2/68	2305	2145	3+	4_o 3+
	Aug. 3/68	0212	0121	2_o	3+ 2_o
	Aug. 3/68	0515	0454	2_o 3+	2_o
Red Deer	May 24/68	0019	0004	3+ 3-	3+ 3-
	May 24/68	0356	0341	3- 3-	3- 3-
Taber	June 19/68	1407	1405	0+ 0+	0+ 0+
Turin	June 17/68	1008	1101	2+ 2_o	2_o 2_o
	June 17/68	1325	1321	2_o 3_o	2_o 3_o
	June 17/68	1814	1551	3_o 2+	3_o 3_o

3.2 Record Characteristics

Since induction coils were used to record the variations in the surface magnetic field, it was difficult to classify pulsations into Pi's and Pc's. The amplitudes of the various period bands were out of proportion since dH/dt was being recorded. However, a close examination of the records indicated that the pulsation events between 2200 hours to 0500 hours LT could be classified mainly as Pi events and those between 0500 hours to 2200 hours LT were mainly Pc events. Examples of the analogue records for the north-south (Hx) and east-west (Hy) components of the magnetic field variations are shown in Figures 3.2 and 3.3.

The vertical component (Hz) of the magnetic field variations was small when compared to the horizontal components for almost all the records. Any appreciable activity usually was confined to periods greater than 300 seconds. Therefore, the polarization ellipses were assumed to lie mainly in the horizontal plane.

The Kp indices are also given in Table IV. The Kp index is a 3 hour index which is designed to measure the "planetary" variations in geomagnetic activity. It has 28

Figure 3.2 Analogue records for May 30, 1968 as recorded at the Observatory and Horse Thief Canyon.

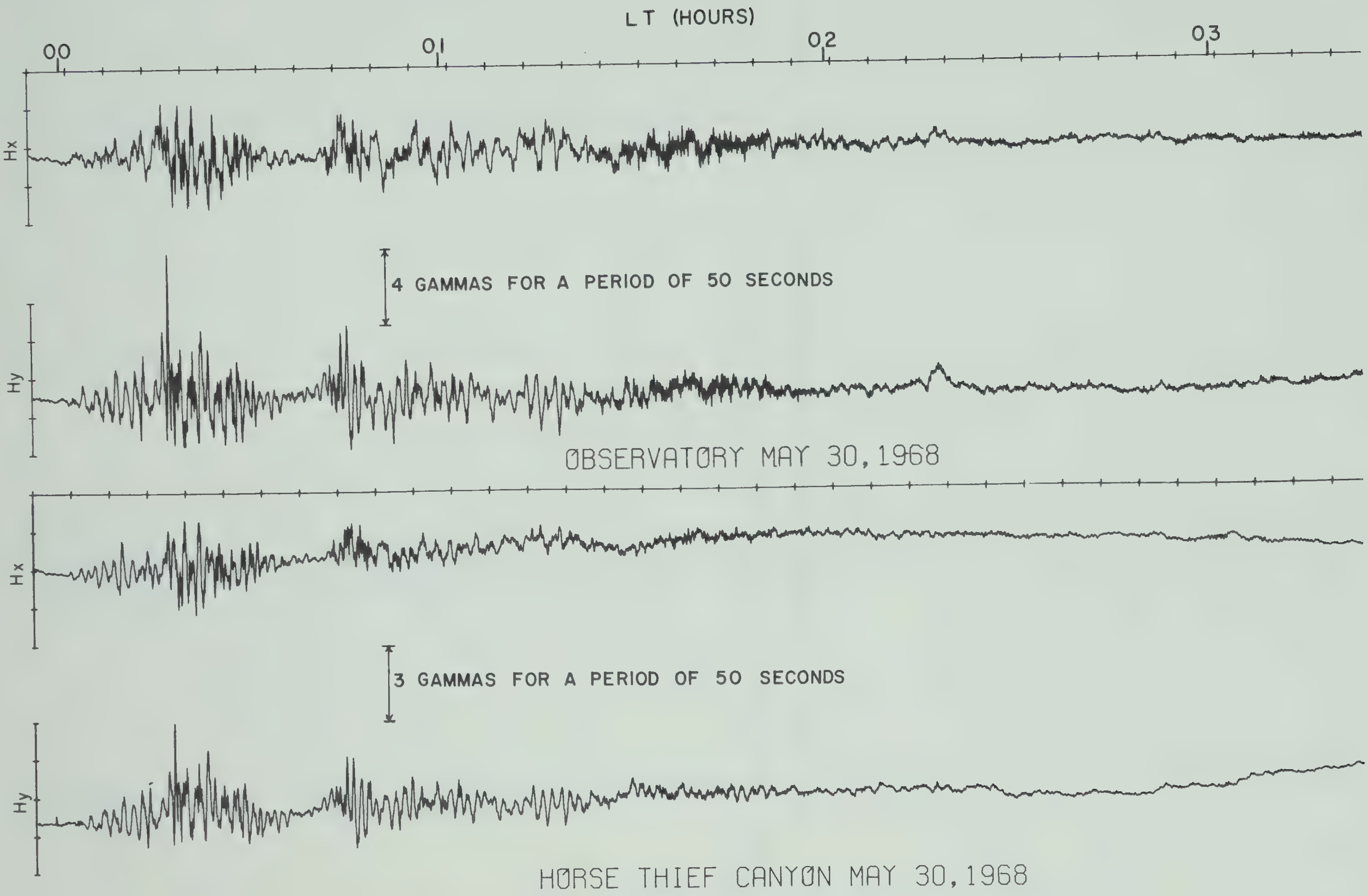
LT (HOURS)
00
01
02
03
Hx
Hy
4 GAMMAS FOR A PERIOD OF 50 SECONDS
OBSERVATORY MAY 30, 1968
Hx
Hy
3 GAMMAS FOR A PERIOD OF 50 SECONDS
HORSE THIEF CANYON MAY 30, 1968

Figure 3.3 Analogue records for August 17, 1968 as recorded at the Observatory and Carrot Creek.

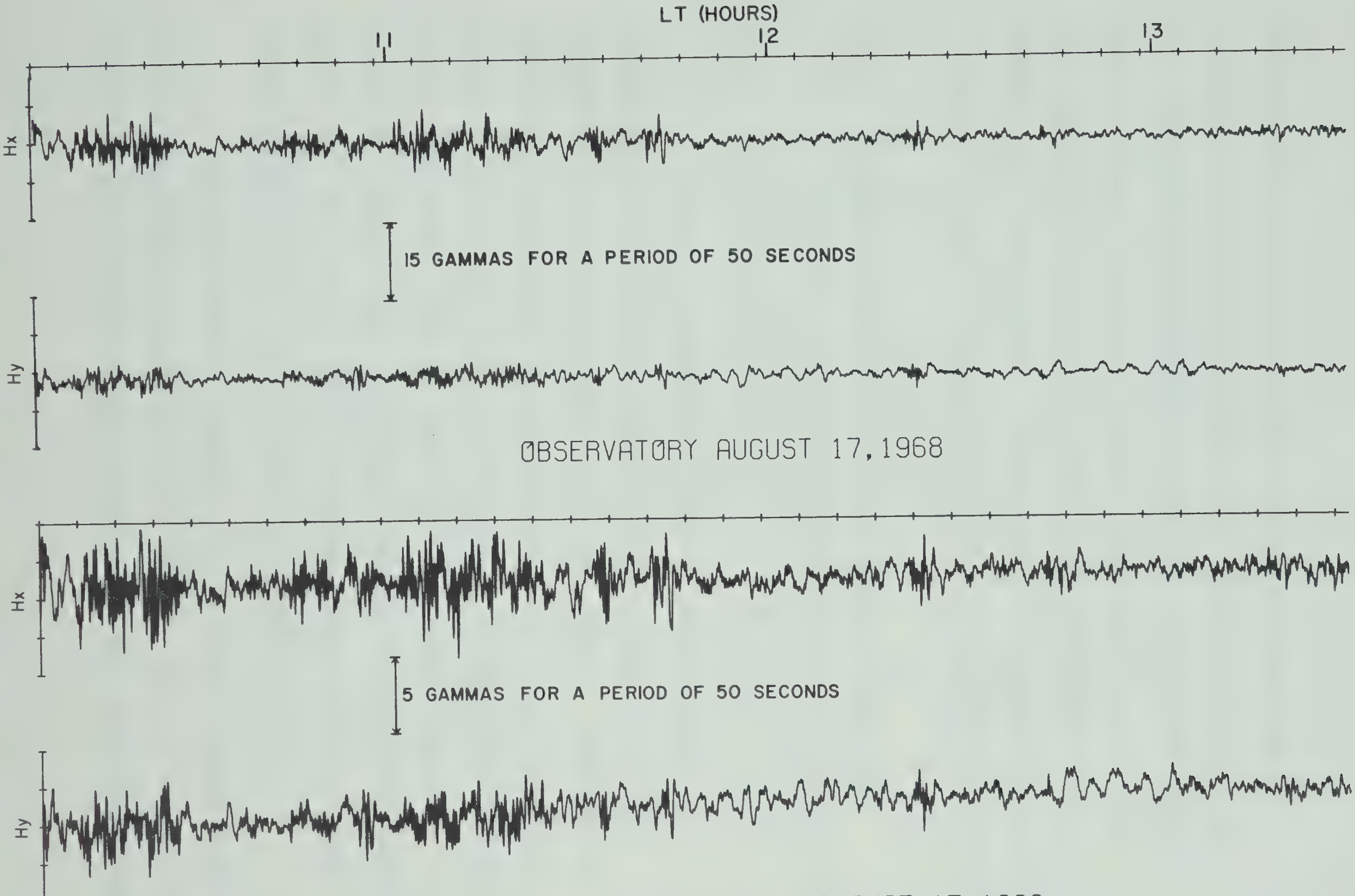

OBSERVATORY AUGUST 17,1968

CARROT CREEK AUGUST 17,1968

grades ranging from 0_o, which denotes exceptional quietness, to 9_o which denotes the most intense storm. As can be seen from Table IV most of the records used were made at times when the Kp index was 2 or greater. Two Kp indices are given if the record spanned two Kp three hour index values. Thus most of the records used represent times of reasonably disturbed magnetic conditions.

3.3 Comparisons Between Simultaneous Field and Observatory Results

3.3.1 Individual Records

A careful comparison between Observatory and simultaneously recorded field station power spectrums showed that they were similar in all cases. Examples of field and Observatory power spectrums for the north-south component (Hx) are shown in Figures 3.4 and 3.5. These power spectrums have not had the instrument response removed. Therefore, they are essentially the prewhitened spectrums and the contours shown are used only to determine the periods at which there were power peaks.

As mentioned in Chapter II, plots of polarization angles were made as functions of time of day and of period. Examples for the field and Observatory are shown in Figures

Figure 3.4 Prewhitened digital sonograms for May 30, 1968 for the Observatory and Horse Thief Canyon.

PREWHITENED DIGITAL SONOGRAM

MAY 30, 1968

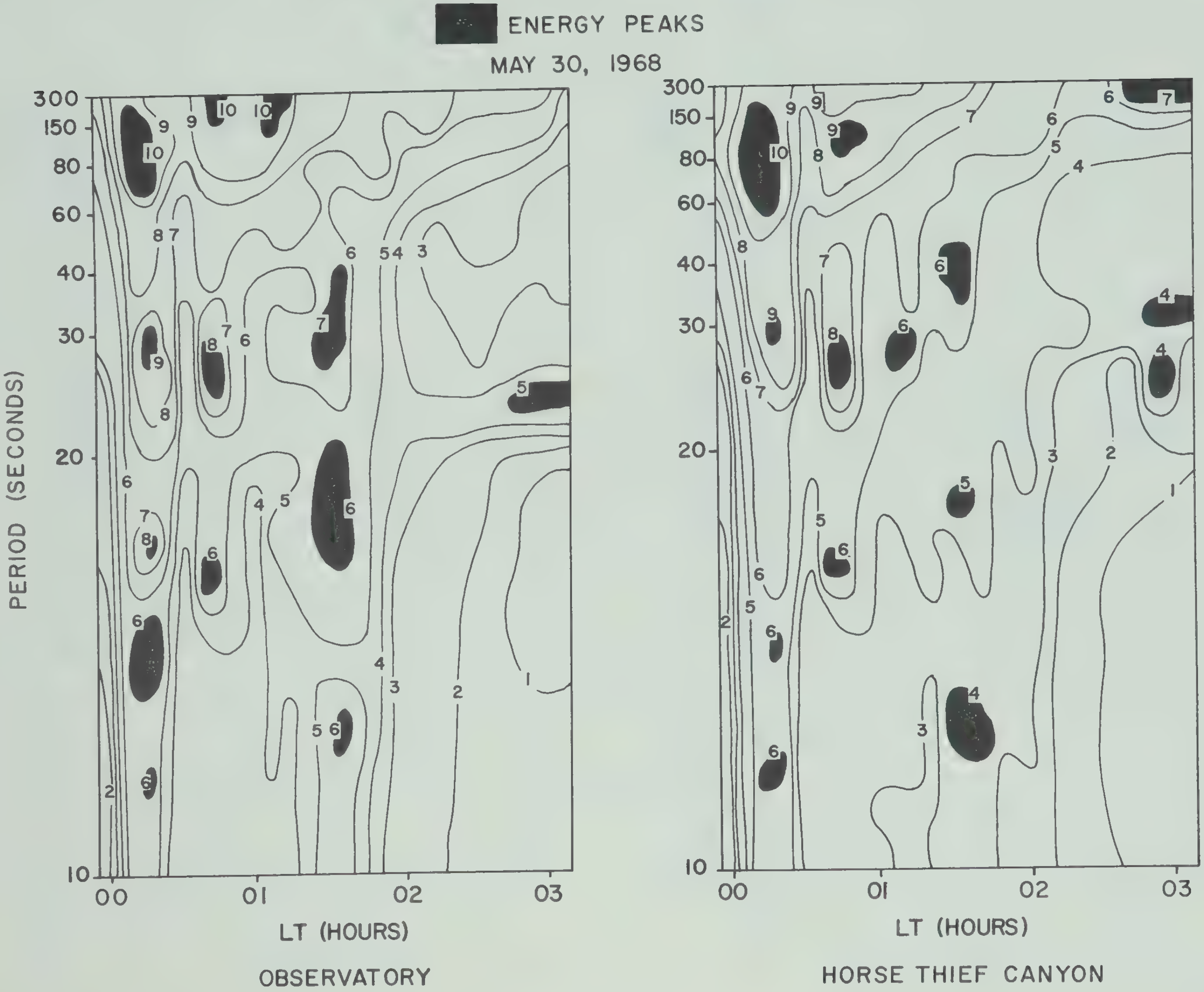

OBSERVATORY

HORSE THIEF CANYON

Figure 3.5 Prewhitened digital sonograms for August 17, 1968 for the Observatory and Carrot Creek.

PREWHITENED DIGITAL SONOGRAM

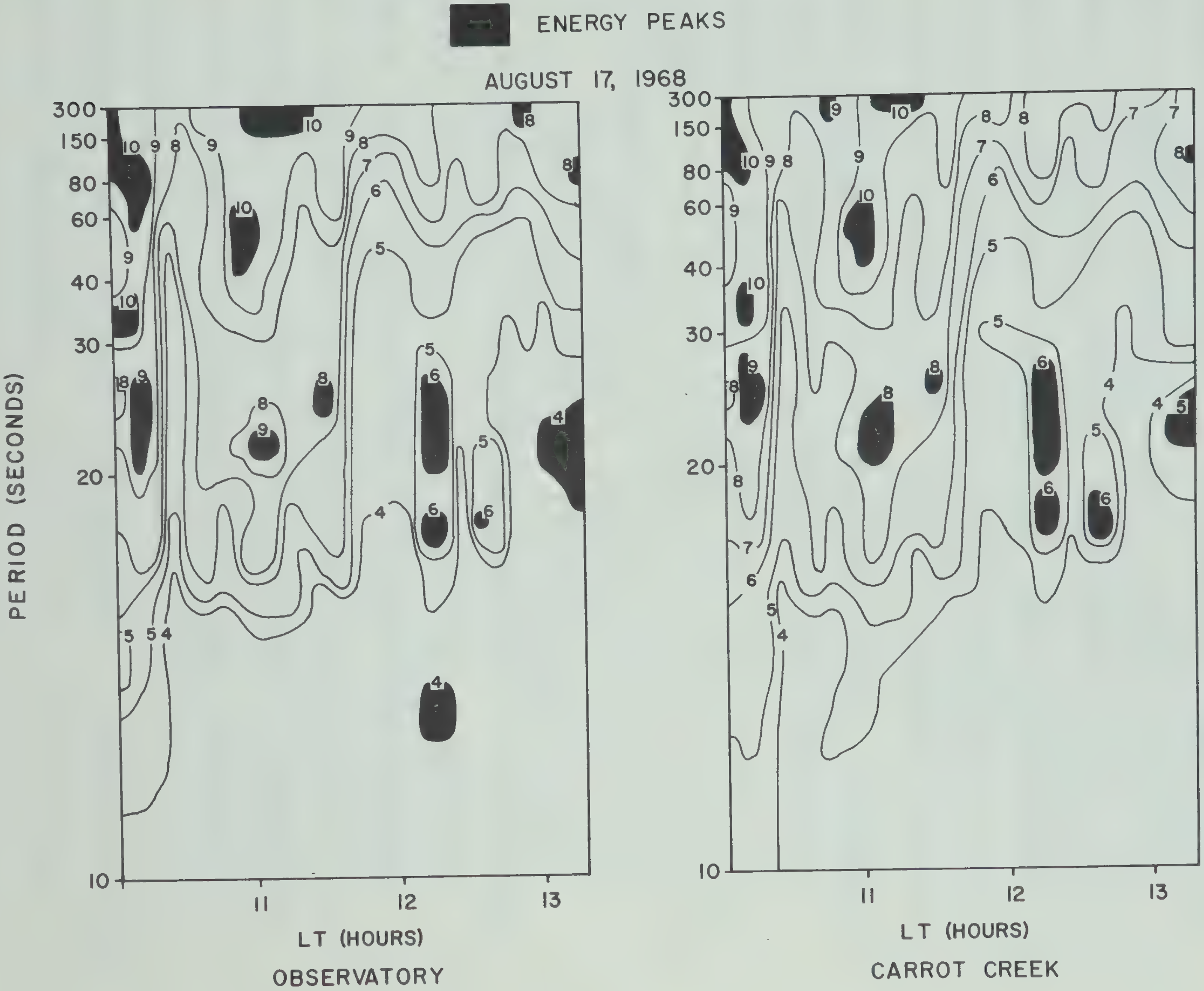

3.6 and 3.7. No consistant visual correlation could be found between these plots and their corresponding power spectrum plots. That is, the polarization angle did not seem to depend on the power present. The angle could remain constant with respect to time whether there was a power spectrum peak present or not. On the other hand, the angle could change rapidly irrespective of the form of the power spectrum plot. This could suggest that the polarization parameters are dependent on local ionospheric conditions above the recording station and not on the source mechanism in the magnetosphere. The source mechanism, then, would be responsible for the amplitude of the pulsation event.

Out of the 43 pairs of field and Observatory records analyzed, 7 pairs showed little or no relationship to each other in their angle of polarization plots. However, angle plots recorded at the same field station at a different time would show a good correlation with the Observatory. This indicates that the lack of correlation is not entirely due to geology of the field station. If one remembers that the power spectrum plots were found to be similar, then this result is probably an indication that while the macrostructure of the pulsation event remains

Figure 3.6 Angle of polarization for May 30, 1968 for the Observatory and Horse Thief Canyon.

ANGLE OF POLARIZATION

MAY 30, 1968

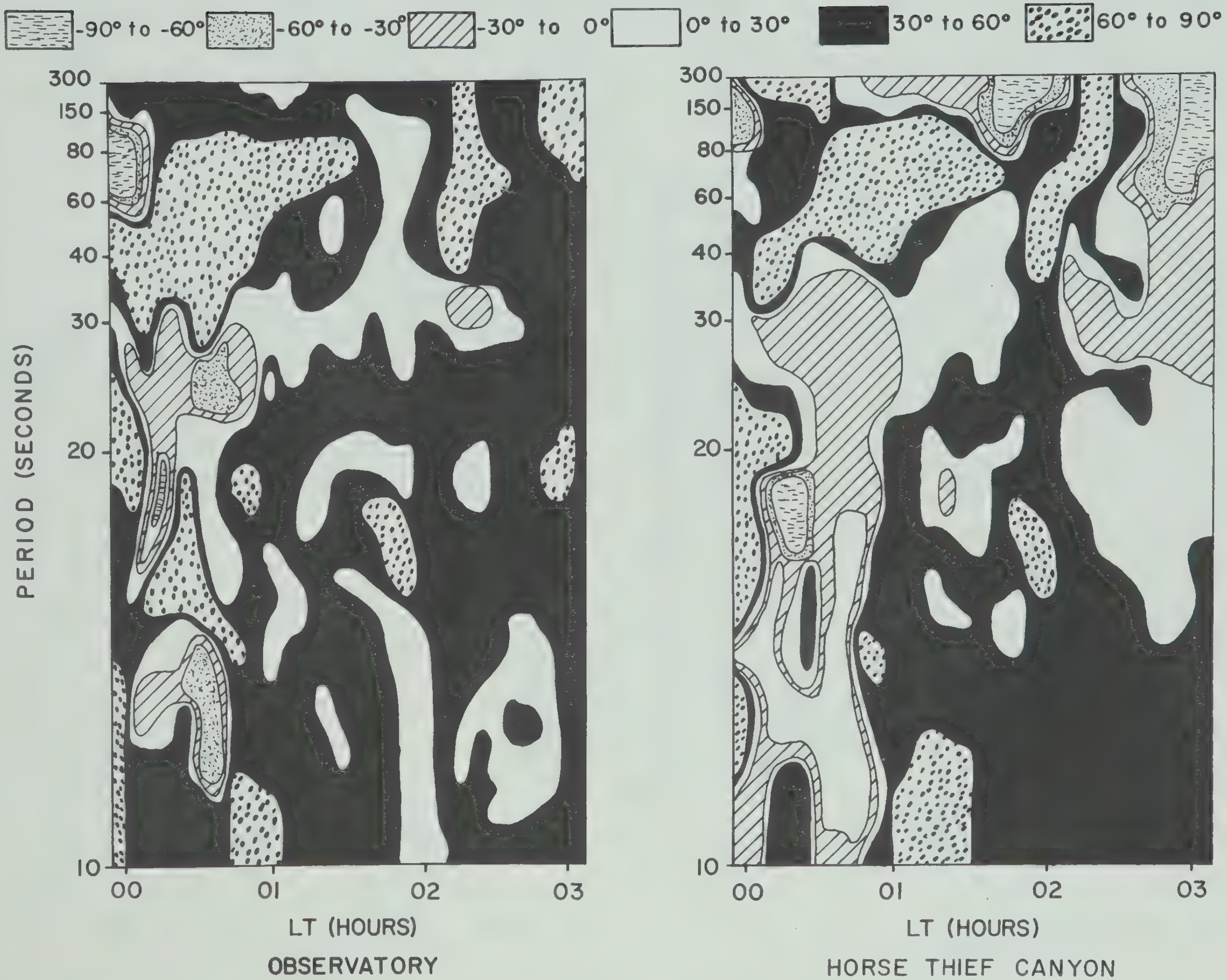

Figure 3.7 Angle of polarization for August 17, 1968 for the Observatory and Carrot Creek.

ANGLE OF POLARIZATION
AUGUST 17, 1968

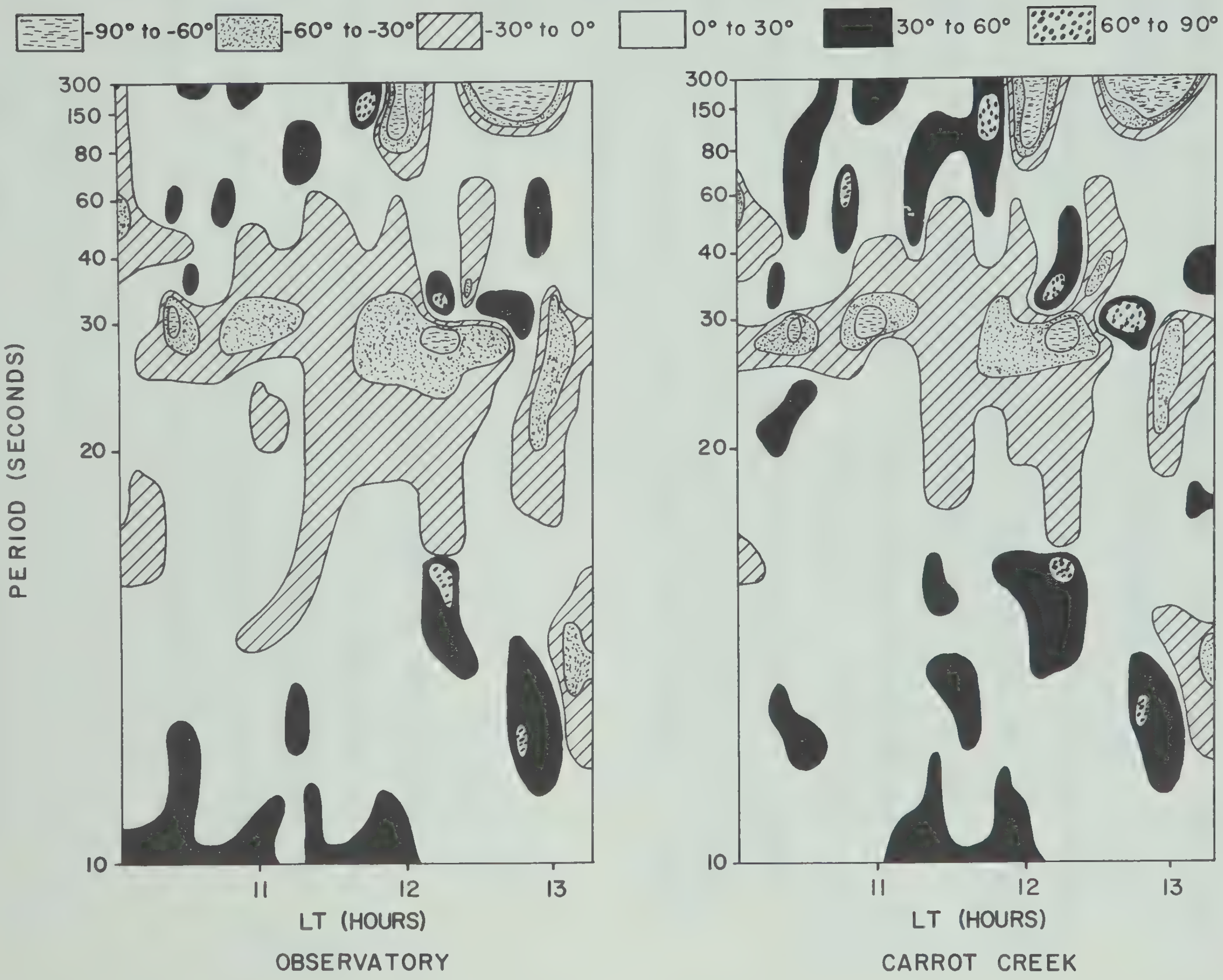

relatively constant over a distance of several hundred kilometers, the phases of the signal can change. This may possibly be due to ionospheric inhomogeneities.

Somewhat the same results appeared when the sense of polarization was considered. Figures 3.8 and 3.9 show examples of the sense as determined from field and Observatory records. Five field and Observatory pairs showed little correlation. That is, the sense would switch from clockwise to counterclockwise polarization independently at each station. Once again, the sense of polarization plots showed little, if any, relationship to the power spectrum plots.

3.3.2 Averaged Results

While each angle of polarization and sense of polarization plot had very interesting characteristics, nothing definite could be said about these polarization parameters in general. Therefore, all the plots were averaged to determine more general characteristics.

(a) Sense of Polarization

The sense of polarization obtained from the Observatory records were averaged to determine the

Figure 3.8 Sense of polarization for May 30, 1968 for the Observatory and Horse Thief Canyon.

SENSE OF POLARIZATION

MAY 30, 1968

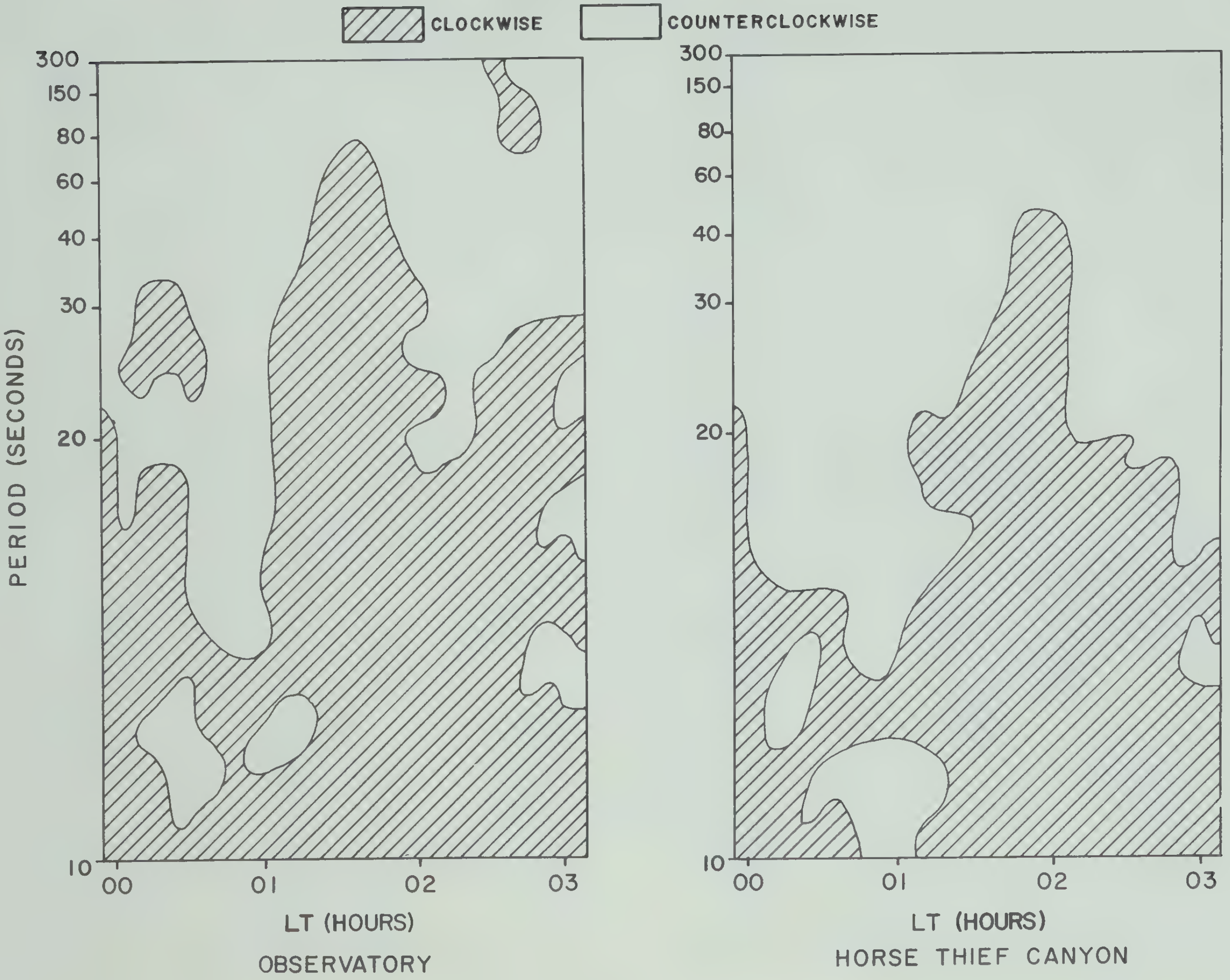

Figure 3.9 Sense of polarization for August 17, 1968 for the Observatory and Carrot Creek.

SENSE OF POLARIZATION

AUGUST 17, 1968

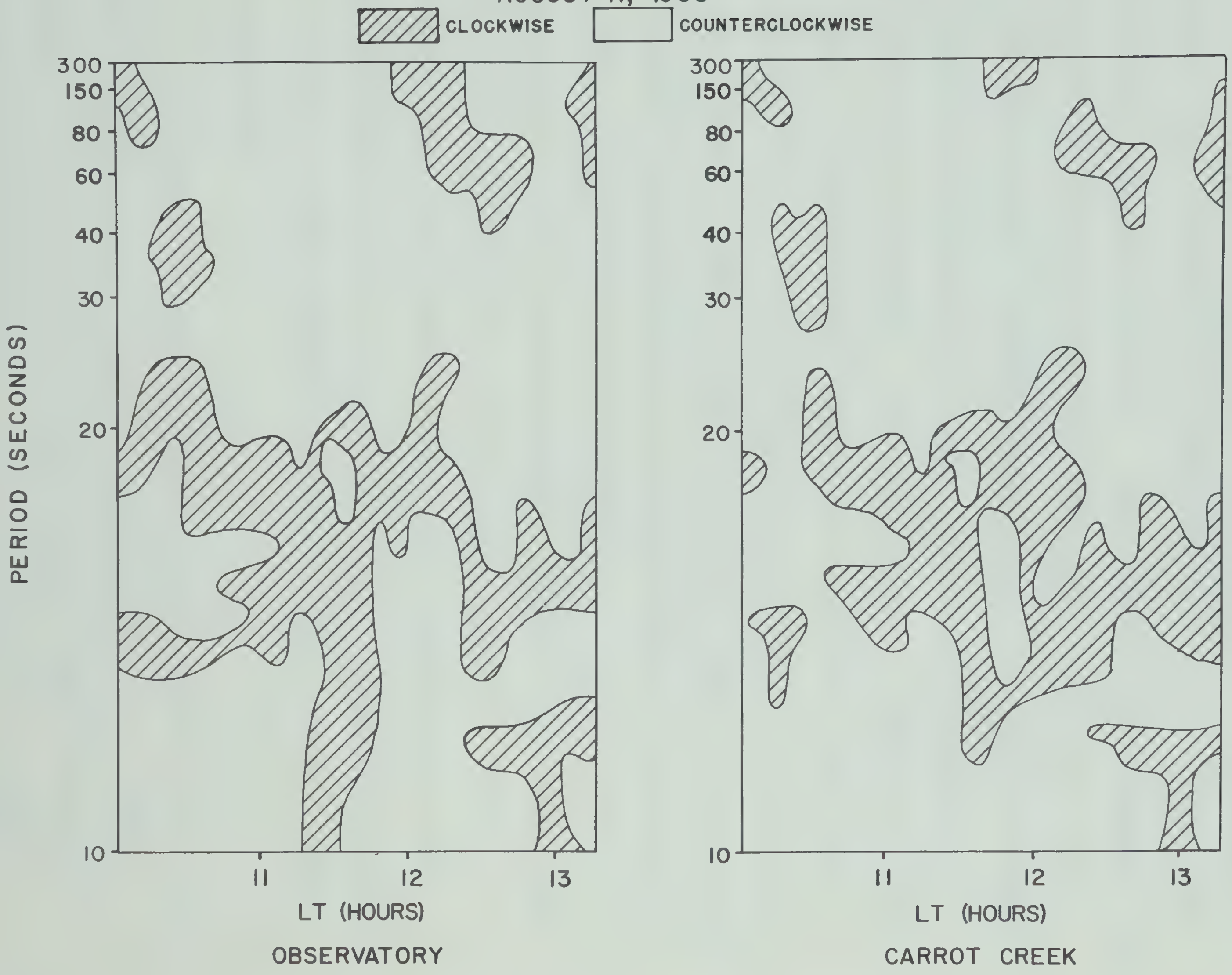

dominant sense as a function of period and time of day. All the plots were sorted into hour intervals according to the time of day at which the records were taken. This was done for each period estimate. (As was shown in Chapter II, the Fast Fourier Transform technique gives discrete autopower and crosspower spectral estimates at certain periods. The polarization parameters were calculated for each of these spectral estimates. The term, period estimate, means the sense of polarization that was calculated from the spectral estimates.) Then, the number of times that the polarization sense was counterclockwise, was divided by the total number of polarization sense estimates to give the percentage of sense estimates that were counterclockwise in an hour interval at a given period. Figure 3.10 shows the result which was obtained. The total number of sense estimates which were used in each hour interval are displayed at the bottom of Figure 3.10. The segmented sections of the contour lines represent the times at which no data were available.

The figure shows that all micropulsation events in the period range from 80 to 273 seconds are 60 to 70% polarized in the counterclockwise sense, except between 1300 hours to 1800 hours LT. The intrusion of counter-

Figure 3.10 Percentage of counterclockwise polarization as a function of time of day and of period. All of the Observatory records were averaged to produce this figure.

PERCENTAGE OF COUNTERCLOCKWISE POLARIZATION
AS A FUNCTION OF TIME AND OF PERIOD FOR THE
OBSERVATORY RECORDS

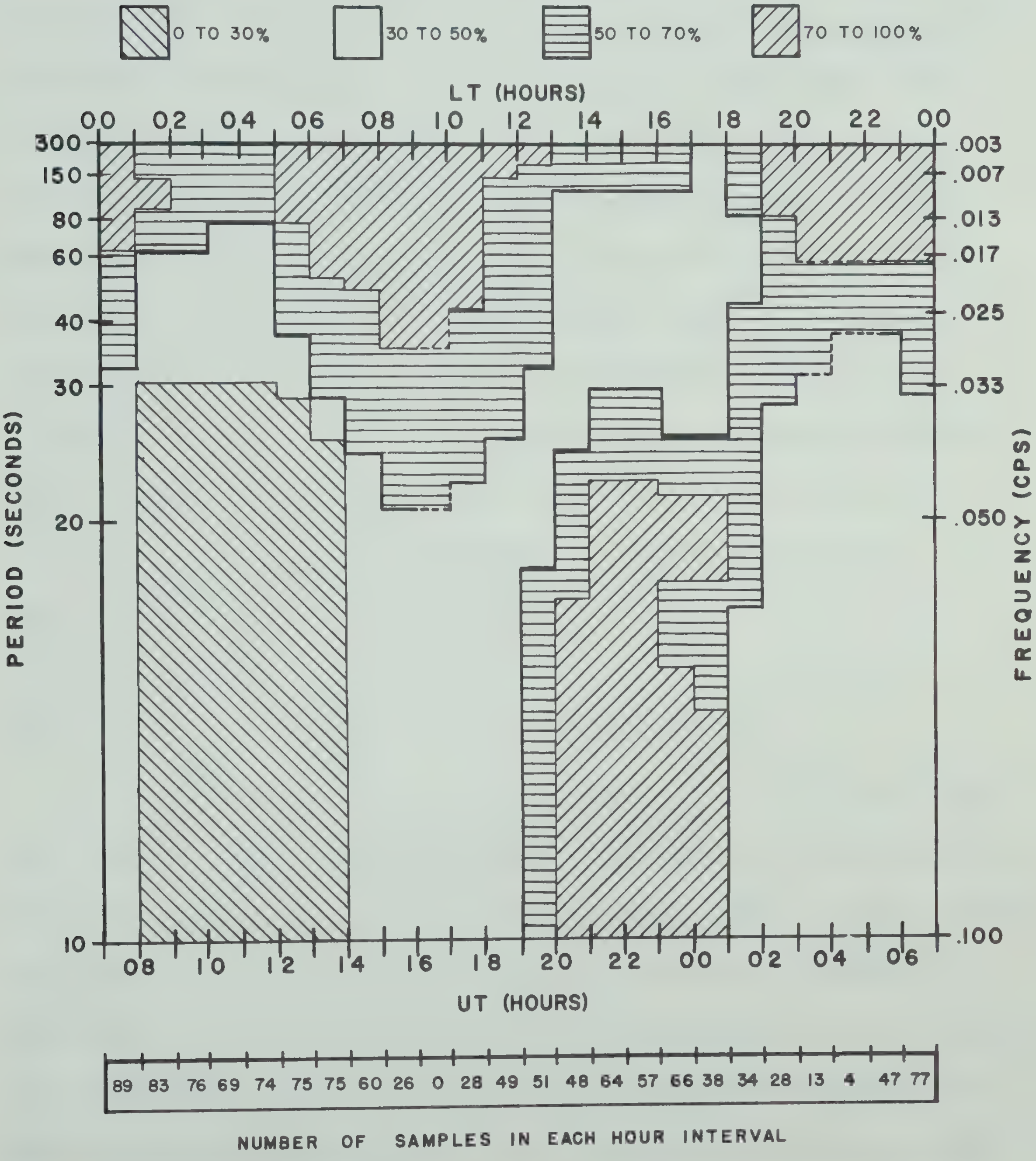

clockwise polarization into shorter period events between 0500 to 1200 hours LT supports Zybin (1967) who found that the sense was 80 to 90% counterclockwise for all micropulsations in the period range from 30 to 1200 seconds in the local morning hours. In the period range above 100 seconds, Figure 3.9 showed that 80 to 90% of the micropulsations events were polarized in the counterclockwise sense in the local morning hours. This also is consistant with the results obtained by Rostoker (1967b) who found that 70% of the Pi2 events had a counterclockwise sense of polarization. If one remembers the predicted inverted sense between the northern and southern hemispheres on the basis of Alvén wave propagation, then, this also agrees with the results of Christoffel and Linford (1966) who found that 61% of the Pi2 events recorded in New Zealand had a clockwise sense of polarization.

Frequencies which correspond to the Pi1 band have 70 to 90% of their contributions polarized in the clockwise direction in the local nighttime hours. This clockwise sense continues until 1100 or 1200 hours LT and then changes abruptly. They then become 60 to 80% counterclockwise polarized. Campbell (1967) states that during the daytime maximum occurrence period of Pc3's, the counterclockwise sense of

polarization predominates. The maximum occurrence period has been found by Jacobs and Sinno (1960b) to peak at 1200 to 1300 hours LT in northern middle latitudes. The results shown in Figure 3.10, then, agree well with Campbell (1967). The sense of polarization corresponding to the Pc4 band is slightly more confused.

Campbell also states that the angle of polarization undergoes a diurnal change with which the sense also changes. No conclusive evidence for this was found as will be seen in part (b) of this section.

(b) Angle of Polarization

Examination of individual plots of angle of polarization versus period and time of day, showed that it was difficult to determine general trends. Therefore a computor program was written to compute the average angles. As was done for the sense of polarization, all the polarization angle estimates from the Observatory records were sorted into hour intervals according to the time of day at which they were recorded. Then, the angle estimates were grouped into 5 period bands which were: 10 to 20 seconds, 20 to 45 seconds, 45 to 68 seconds, 68 to 136 seconds, and 136 to 273 seconds. The angle estimates for

each period were then averaged to give the average angle in a given period band. These averaged angle estimates over a given period band were then further sorted into angle groups. There were 12 angle groups ranging from -90° (i.e. geographic west) to +90° (i.e. geographic east) in increments of 15°. The percentage of the angles falling in each of the 12 angle groups was displayed on histograms and are shown in Figure 3.11 through Figure 3.15. Figures 3.11a and 3.11b are for the period band 136 to 273 seconds, 3.12a and 3.12b for 68 to 136 seconds, 3.13a and 3.13b for 45 to 68 seconds, 3.14a and 3.14b for 20 to 45 seconds, and Figures 3.15a and 3.15b are for the period band 10 to 20 seconds. The records from the 13 field locations were averaged together in a similar manner and the results are displayed beside the Observatory histograms for comparison. It must be remembered that each field station record corresponds to an Observatory record. Therefore, any differences between the field and Observatory histograms are mainly due to changes in geoelectric structure of each field station and changes in the signal as it propagates from the source to the two recording stations.

An examination of Figure 3.11 through to Figure 3.15, for the Observatory, immediately reveals one interest-

Figure 3.11a and Figure 3.11b

Histograms for the angle of polarization averaged over hour intervals for the Observatory and field records. These figures are for the 136 to 273 second period band.

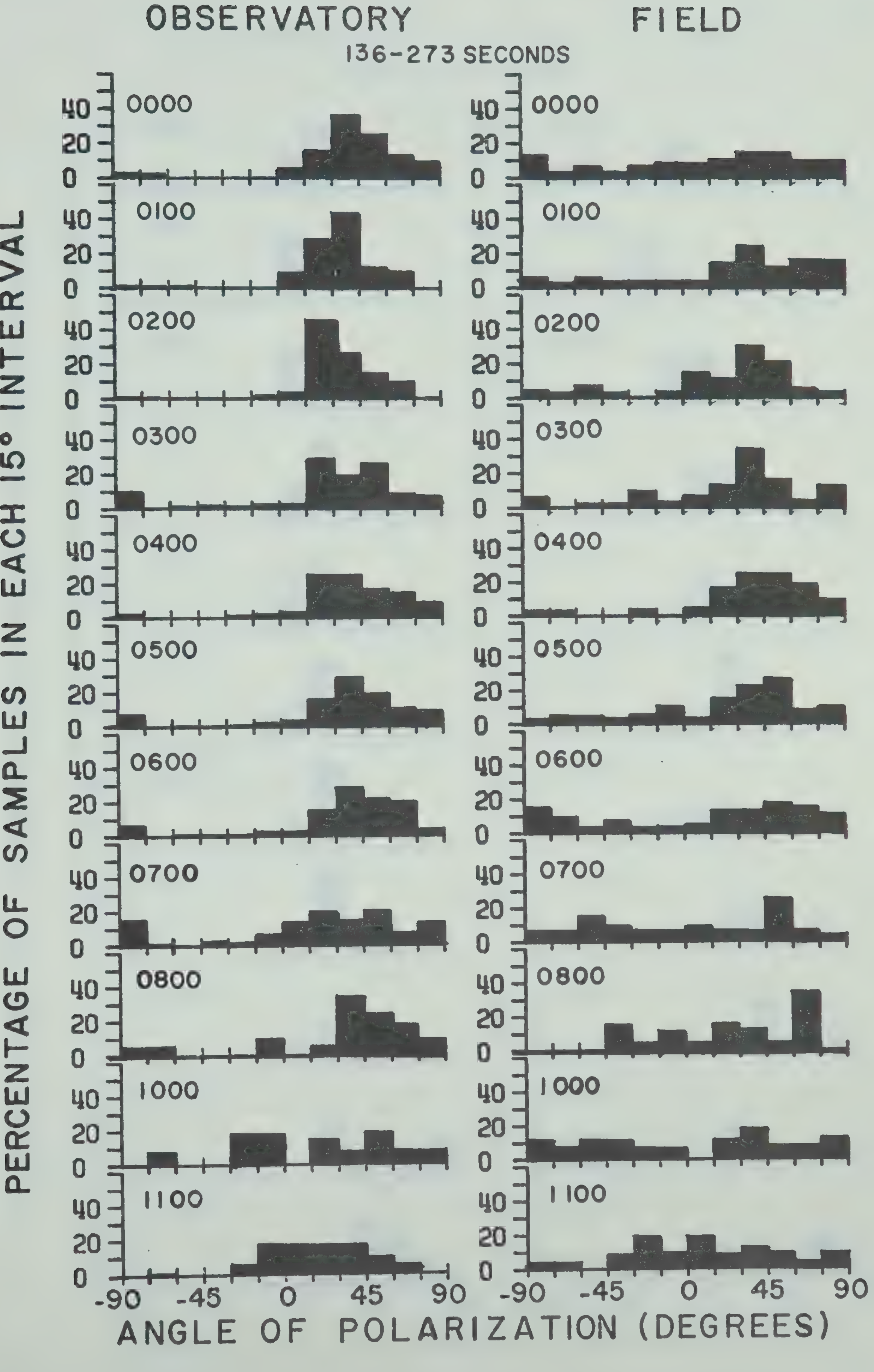
OBSERVATORY
FIELD
136-273 SECONDS
PERCENTAGE OF SAMPLES IN EACH 15° INTERVAL
0000
0100
0200
0300
0400
0500
0600
0700
0800
1000
1100
40
20
0
-90
-45
0
45
90
ANGLE OF POLARIZATION (DEGREES)

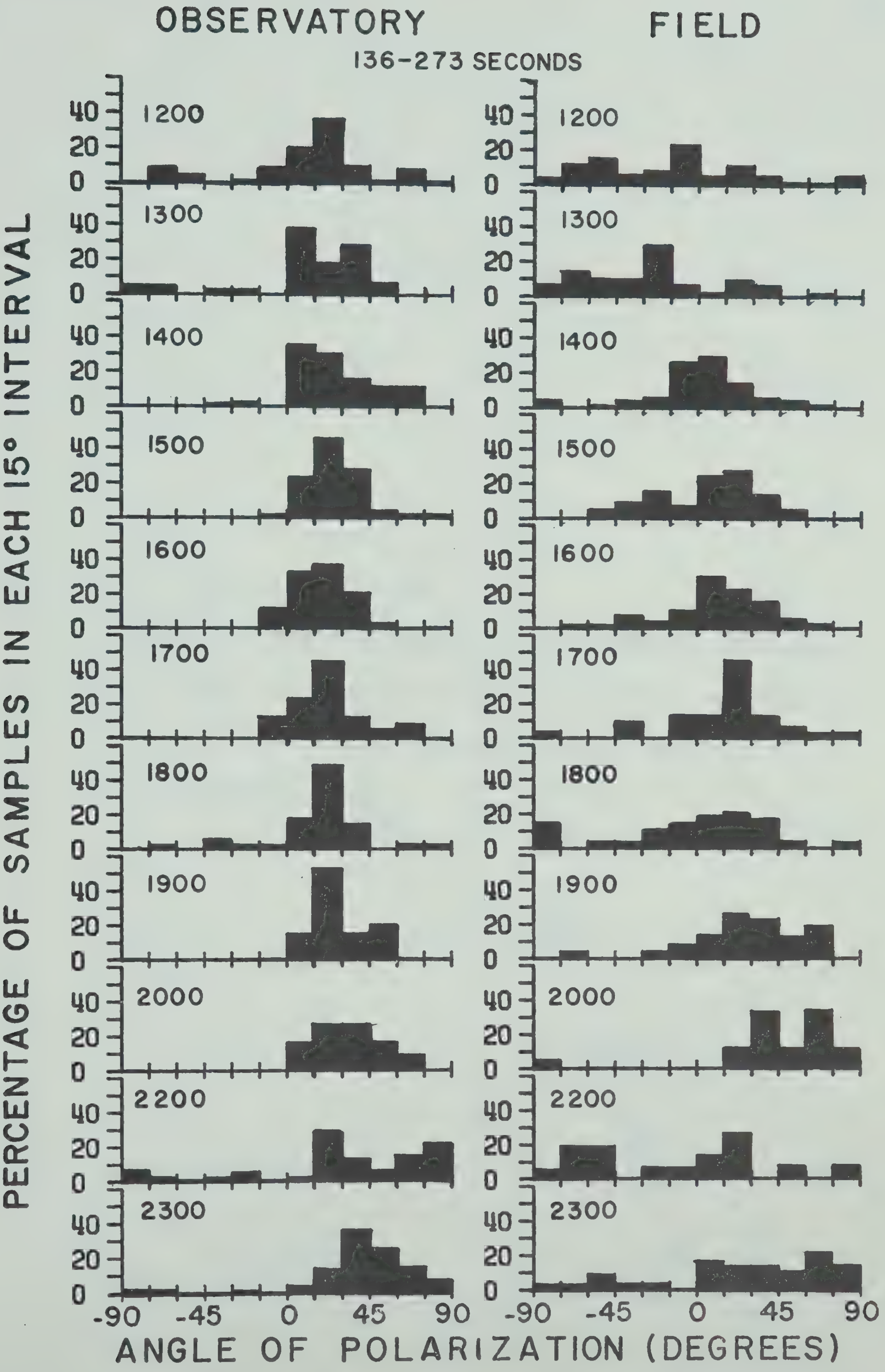
OBSERVATORY
FIELD
136-273 SECONDS
1200
1300
1400
1500
1600
1700
1800
1900
2000
2200
2300
0
20
40
-90
-45
0
45
90
PERCENTAGE OF SAMPLES IN EACH 15° INTERVAL
ANGLE OF POLARIZATION (DEGREES)

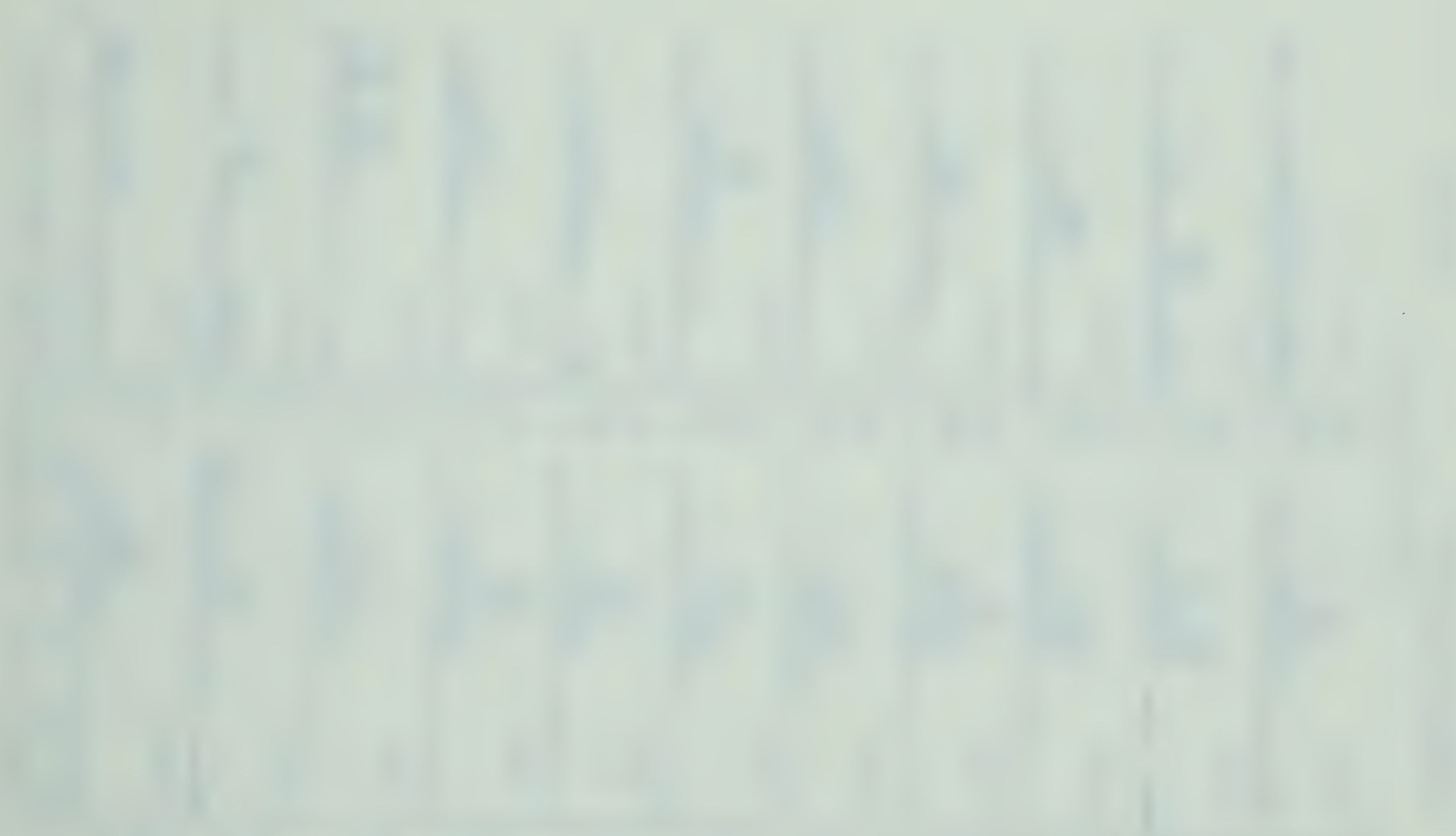

[illegible]

Figure 3.12a and Figure 3.12b

Histograms for the angle of polarization averaged over hour intervals for the Observatory and field records. These figures are for the 68 to 136 second period band.

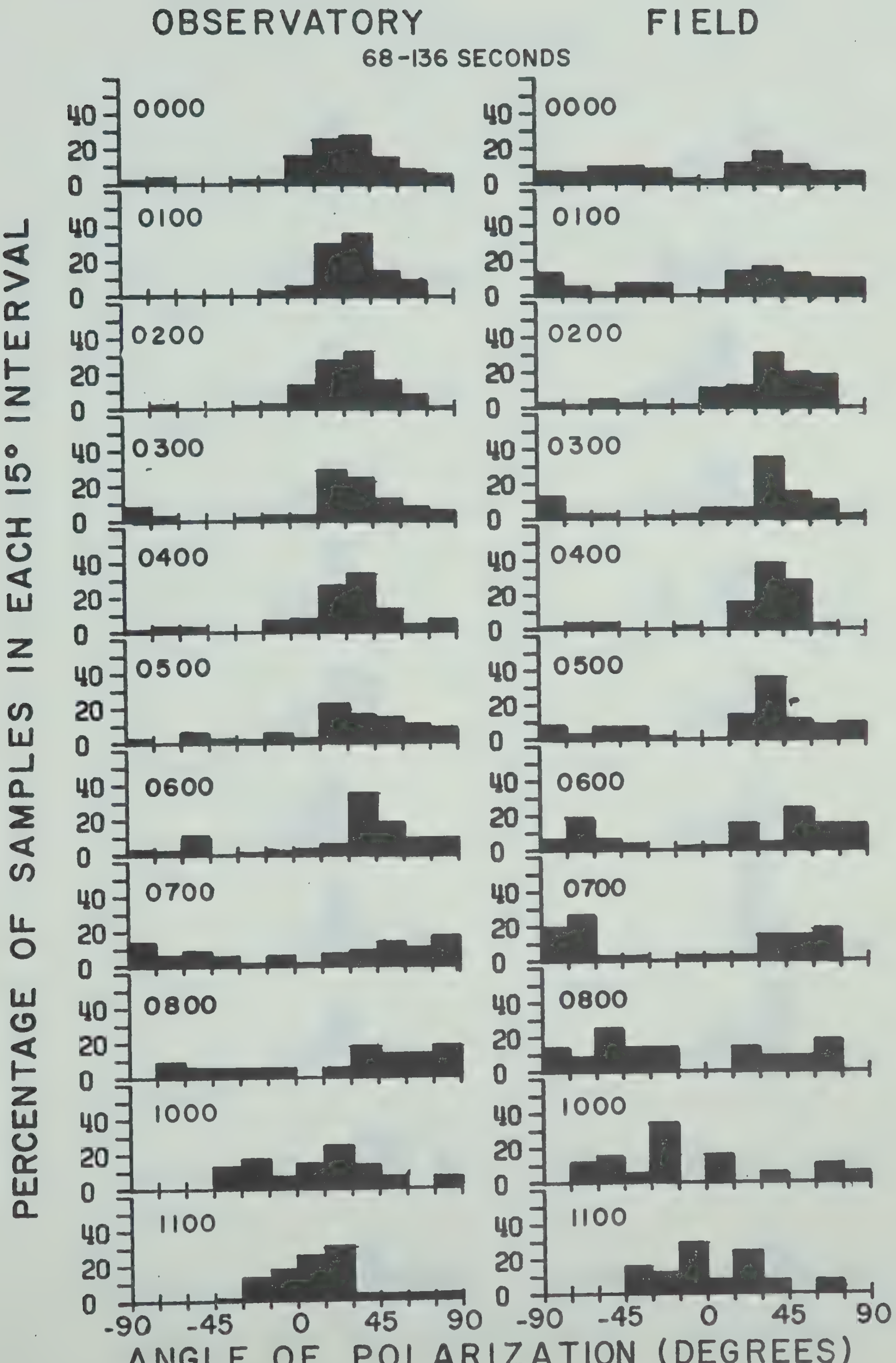

OBSERVATORY

FIELD

68-136 SECONDS

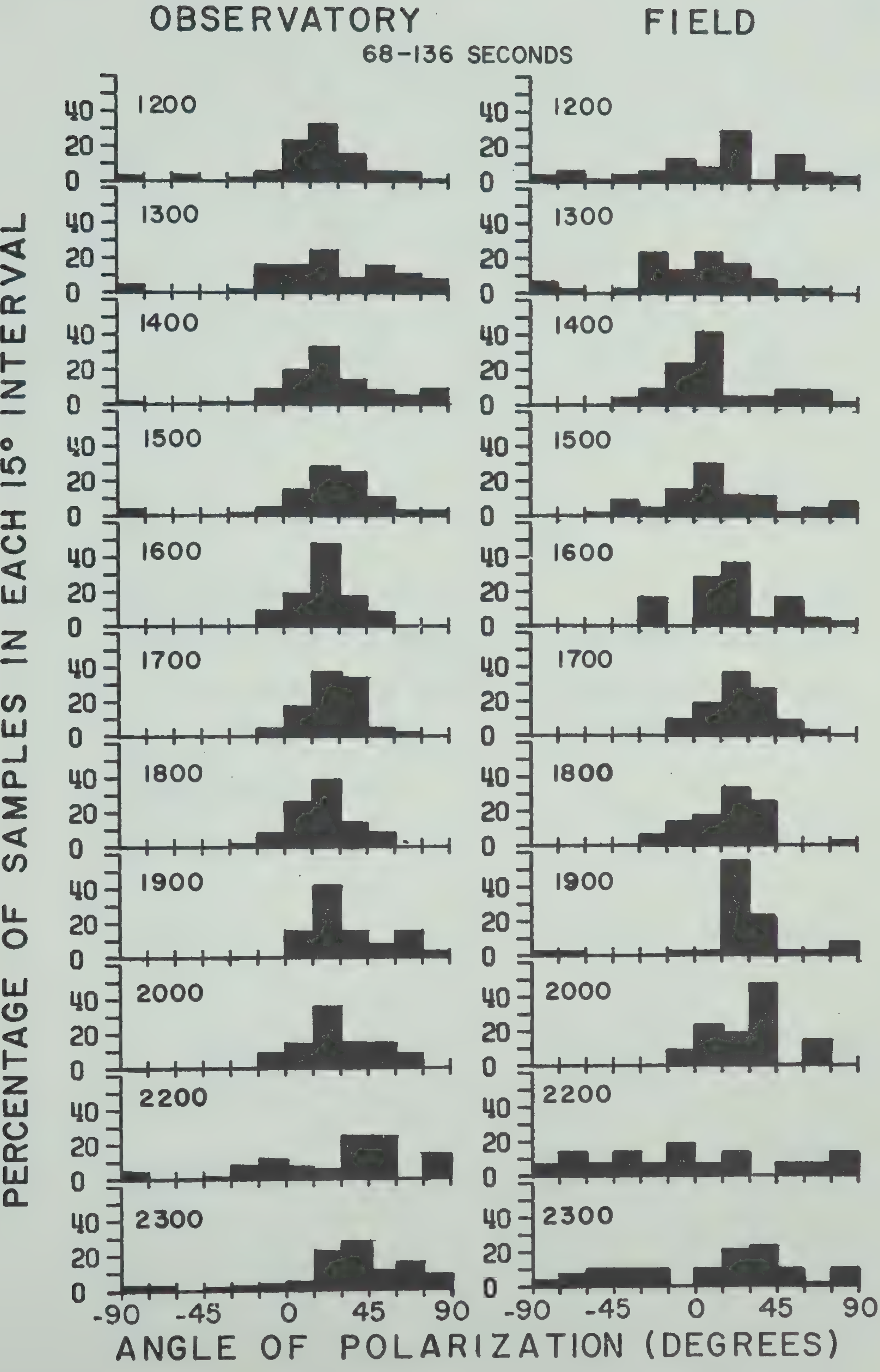
OBSERVATORY
FIELD
68-136 SECONDS
PERCENTAGE OF SAMPLES IN EACH 15° INTERVAL
1200
1300
1400
1500
1600
1700
1800
1900
2000
2200
2300
0
20
40
-90
-45
0
45
90
ANGLE OF POLARIZATION (DEGREES)

[illegible]

Figure 3.13a and Figure 3.13b

Histograms for the angle of polarization averaged over hour intervals for the Observatory and field records. These figures are for the 45 to 68 second period band.

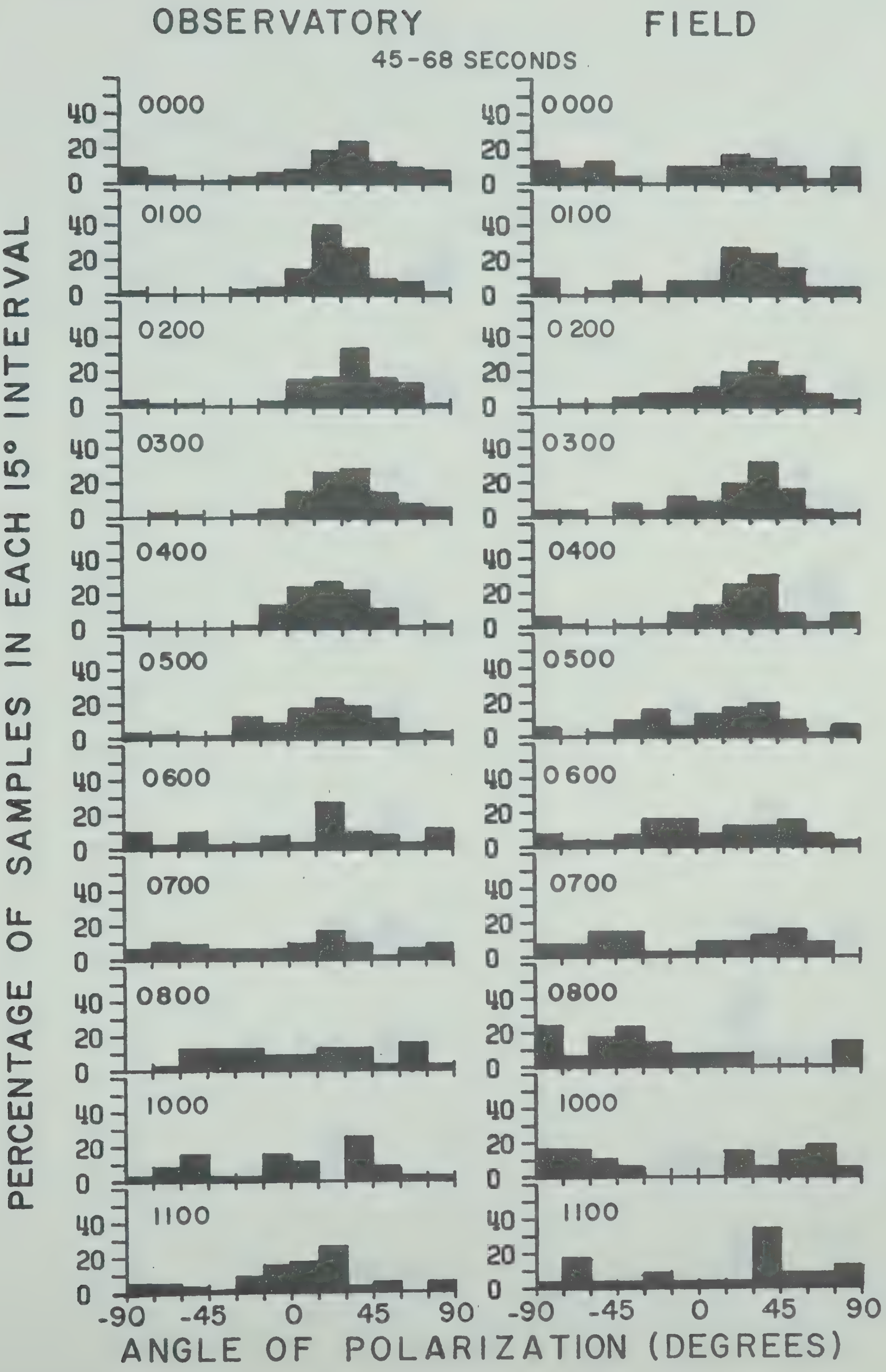
OBSERVATORY
FIELD
45-68 SECONDS
0000
0100
0200
0300
0400
0500
0600
0700
0800
1000
1100
40
20
0
-90
-45
0
45
90
PERCENTAGE OF SAMPLES IN EACH 15° INTERVAL
ANGLE OF POLARIZATION (DEGREES)

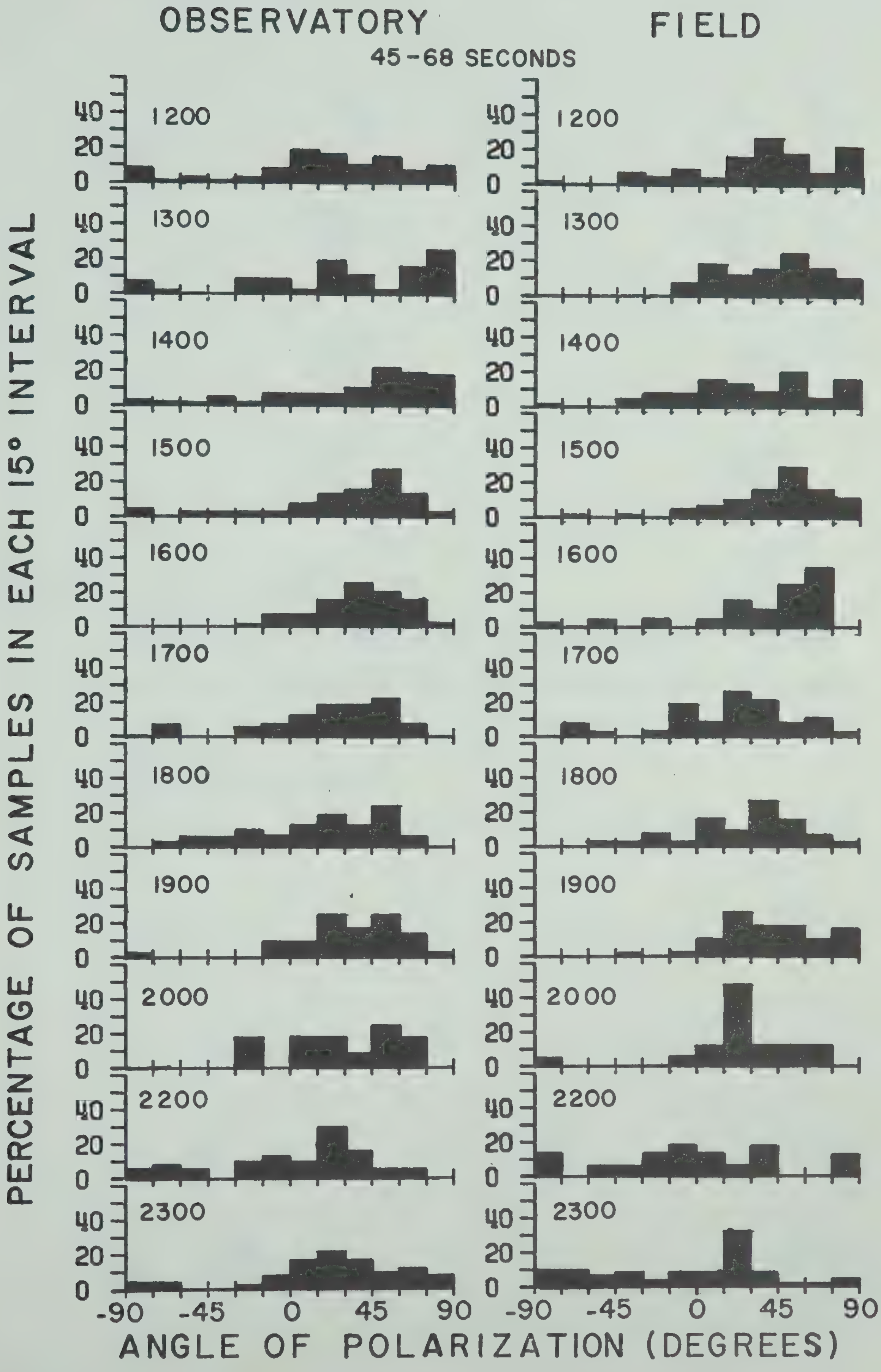
OBSERVATORY
FIELD
45-68 SECONDS
1200
1300
1400
1500
1600
1700
1800
1900
2000
2200
2300
0
20
40
-90
-45
0
45
90
PERCENTAGE OF SAMPLES IN EACH 15° INTERVAL
ANGLE OF POLARIZATION (DEGREES)

Figure 3.14a and Figure 3.14b

Histograms for the angle of polarization averaged over hour intervals for the Observatory and field records. These figures are for the 20 to 45 second period band.

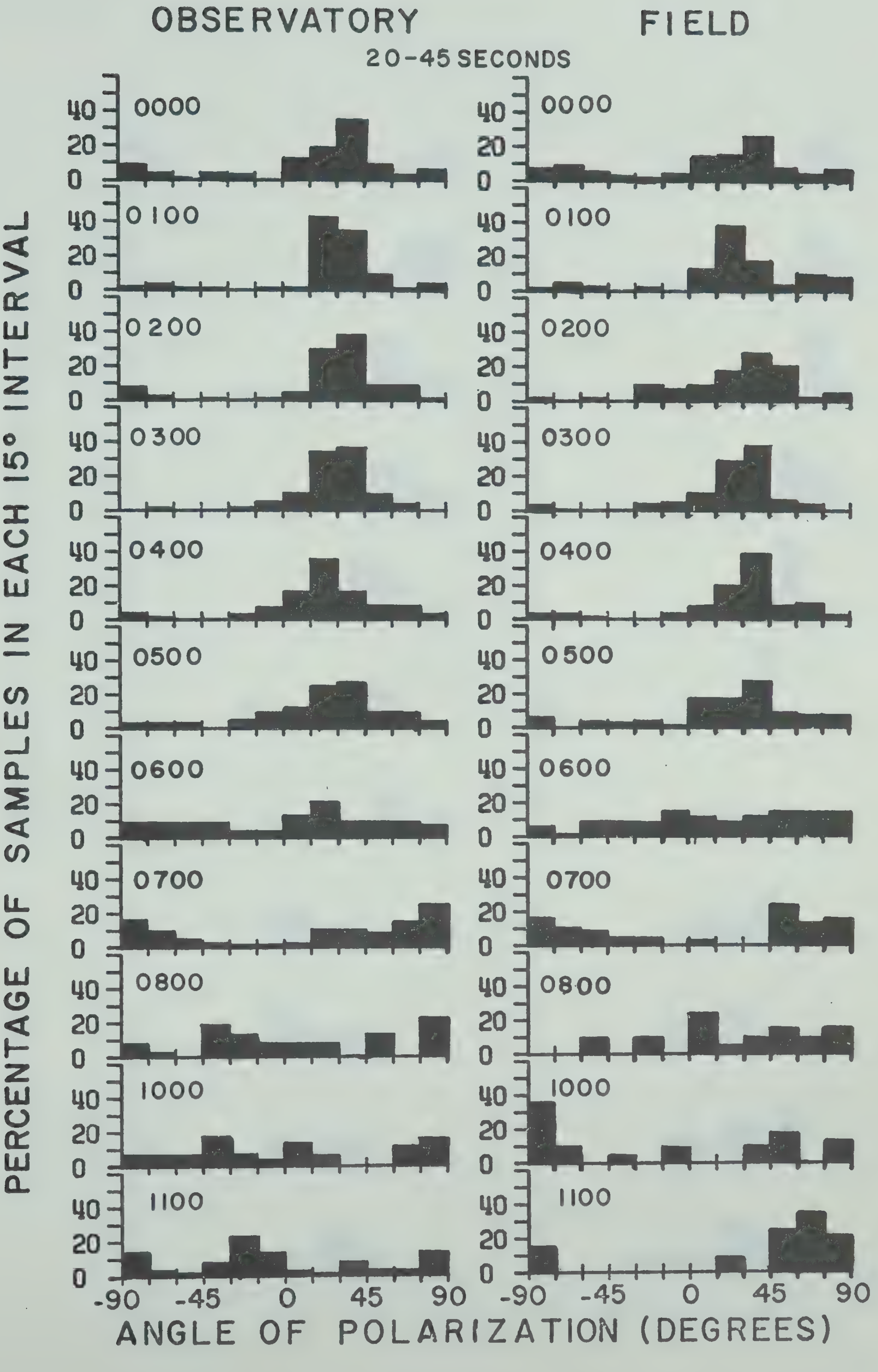
OBSERVATORY
FIELD
20-45 SECONDS
PERCENTAGE OF SAMPLES IN EACH 15° INTERVAL
0000
0100
0200
0300
0400
0500
0600
0700
0800
1000
1100
0
20
40
-90
-45
0
45
90
ANGLE OF POLARIZATION (DEGREES)

[illegible]

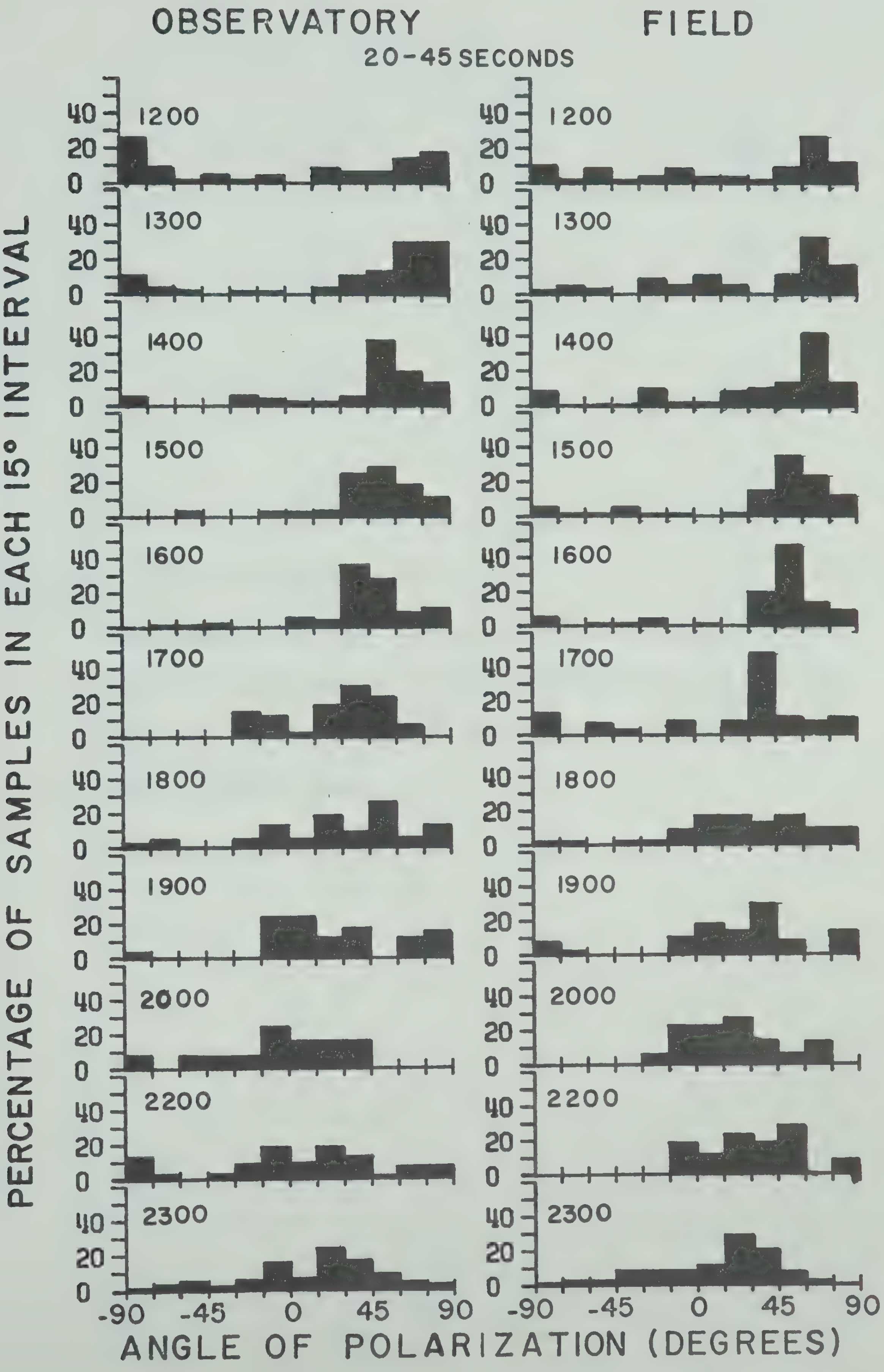
OBSERVATORY
FIELD
20-45 SECONDS
PERCENTAGE OF SAMPLES IN EACH 15° INTERVAL
1200
1300
1400
1500
1600
1700
1800
1900
2000
2200
2300
0
20
40
-90
-45
0
45
90
ANGLE OF POLARIZATION (DEGREES)

[illegible]

Figure 3.15a and Figure 3.15b

Histograms for the angle of polarization averaged over hour intervals for the Observatory and field records. These figures are for the 10 to 20 second period band.

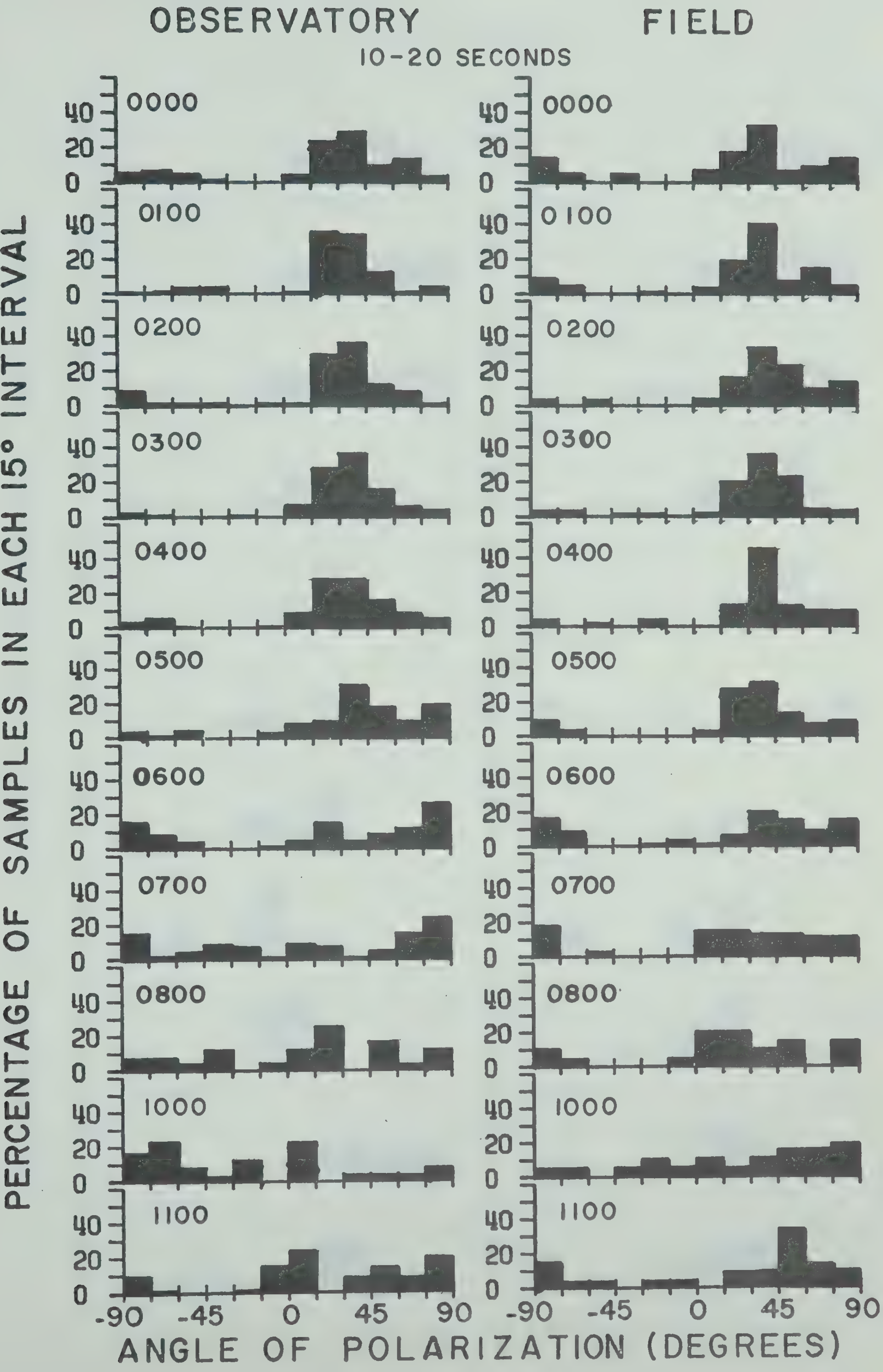OBSERVATORY
FIELD
10-20 SECONDS
PERCENTAGE OF SAMPLES IN EACH 15° INTERVAL
0000
0100
0200
0300
0400
0500
0600
0700
0800
1000
1100
0
20
40
-90
-45
0
45
90
ANGLE OF POLARIZATION (DEGREES)

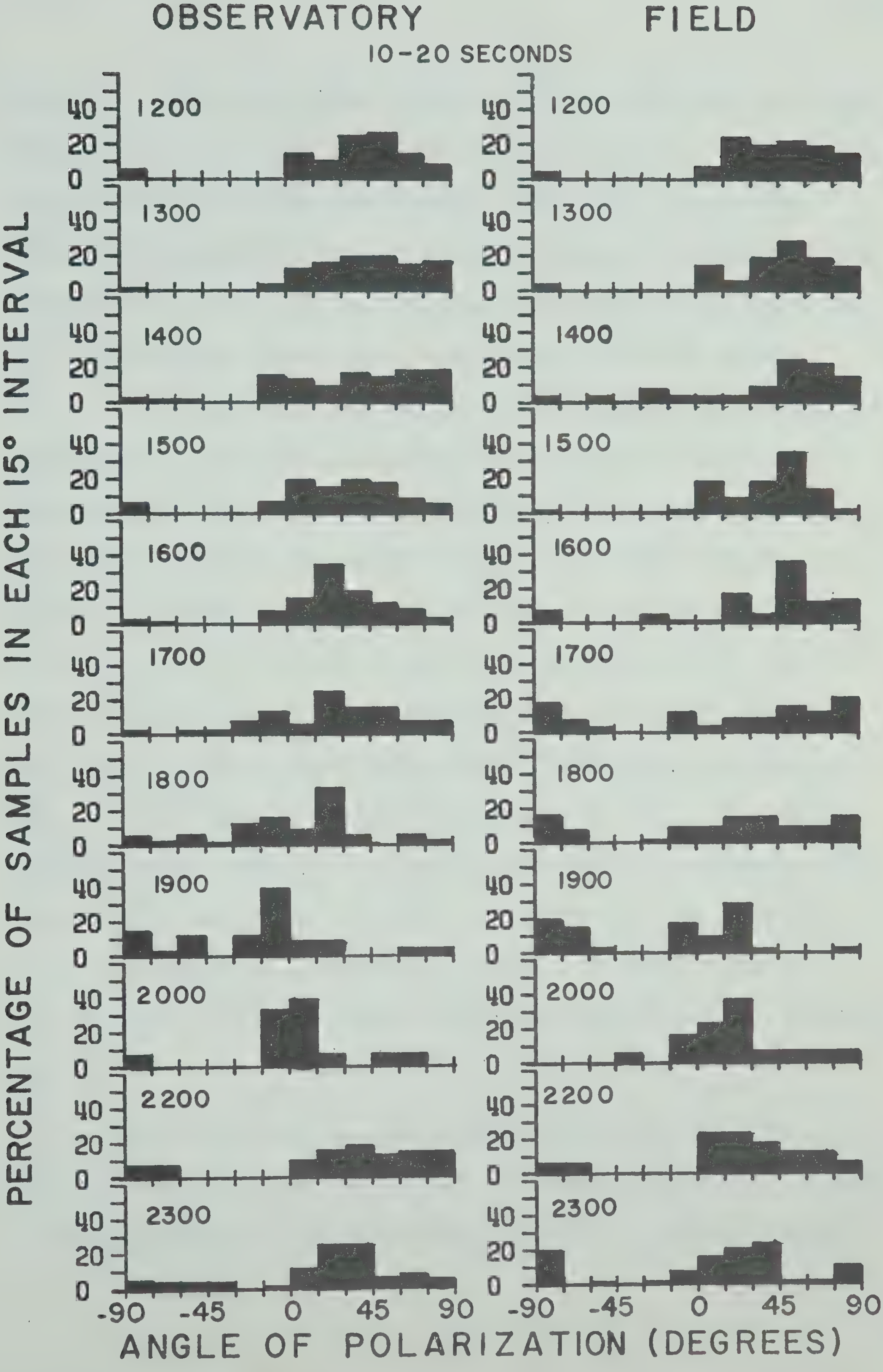
OBSERVATORY
FIELD
10-20 SECONDS
1200
1300
1400
1500
1600
1700
1800
1900
2000
2200
2300
0
20
40
-90
-45
0
45
90
PERCENTAGE OF SAMPLES IN EACH 15° INTERVAL
ANGLE OF POLARIZATION (DEGREES)

ing fact. The major axis of the polarization ellipse falls predominately between 0° to 60° east of north. This result could be explained in three ways. It could be due to geological structures situated in the near vicinity of the Observatory. However, an examination of the corresponding field histograms shows that they also have this general trend. Therefore, if the angle of polarization is being influenced by geologic structure it must be a much more extended feature. The Rocky Mountain Range makes an angle of roughly 45°W of geographic north (see Figure 3.1). Zybin (1967) made the observation that the major axis of the polarization ellipse tends to be perpendicular to the strike of major geological features. This might explain, then, why the field and Observatory histograms display an angle of polarization lying between 0° to 60°. The third explanation is that the polarization angle is aligning with the magnetic meridian. At the Observatory, the magnetic meridian is 23°E of geographic north. Several workers (i.e. Campbell (1967)) have noted that polarization ellipses have tended to be aligned in this fashion for Pc5 events.

A closer look at the histograms revealed more features. All of the histograms for the Observatory tended to have an angle of polarization in the 15° to 60° range in

the local night hours (2300 hours to 0500 hours LT). The histograms seem to become more spread out and scattered in the hours between 0600 hours and 1100 hours LT. This corresponds roughly to the intrusion of counterclockwise polarization into lower periods as is displayed in Figure 3.10.

In Figure 3.11b (273 to 136 second period band) and Figure 3.12b (136 to 68 second period band) the peaks in the histogram seem to lie in the 0° to 30° range between 1200 hours to 2000 hours LT. Between 2000 hours and 2300 hours LT they swing to their nighttime position of 15° to 60°.

The histograms representing the 68 to 10 second period pulsations in the time interval between 1200 hours and 2000 hours LT are more complex. This complex form is also evident in Figure 3.10 for the sense of polarization.

Thus, it seems that for the longer periods (68 seconds to 273 seconds) the angle of polarization lies between 15° to 60° in the local night hours. In the morning hours (0600 hours to 1100 hours LT) the situation is confused. However, between 1200 hours and 2000 hours LT the angle is between 0° to 30°. Then between 2000 hours and 2300 hours LT there is a clockwise swing in the angle

back to its nighttime direction.

(c) Degree of Polarization and Ellipticity

In Chapter II the degree of polarization was defined as the ratio of the polarized signal intensity to the total signal intensity. An averaging process, similar to the one used to obtain Figure 3.10 was carried out. The result showed that on the average, the signal is 65 to 75% polarized for all periods and at all times of the day. Similar results were found from an analysis of the field records.

Again, the same averaging process was applied to the ellipticity values obtained from Observatory records. It was found that, on the average, micropulsation events have a ratio of minor to major axis of 0.2 to 0.4. Thus it can be expected that polarization ellipses will be quite elongated. Similar results were found for the field data.

CHAPTER IV

CONCLUSIONS AND SUGGESTIONS FOR FURTHER RESEARCH

4.1 Conclusions

In this work, methods were developed to analyse the polarization characteristics of geomagnetic micropulsations utilizing large amounts of data. While results from individual records were superficially interesting, more conclusive trends were obtained by using statistical averages. The individual records did show however, that very similar polarization results could be obtained from simultaneous field and Observatory records.

The averaged sense of polarization values indicate that micropulsations in the period range from 30 to 273 seconds were predominantly polarized in the counterclockwise sense except between 1300 hours to 1800 hours LT. For micropulsations with periods below 30 seconds the polarization sense is different than for the longer periods in that there is a semi-diurnal variation in the sense. The sense goes from being predominantly clockwise in the local morning hours centered at 03:30 to strongly counterclockwise in the afternoon hours centered at 15:30. It

may be further noted that these times correspond to those in which the longer period micropulsations are less strongly counterclockwise polarized.

The angles of polarization were also averaged and the results showed that the bulk of the angles lay between 0° to 60° east of north. The strong similarity between the field and Observatory stations indicates that local geology is not a dominant factor in determining the angle of polarization. Thus the observed angle of polarization may be attributed to the source of micropulsations or to regional geologic trends (such as the Rocky Mountains).

The average angle in the local night hours lay between 15° to 60° east of north. In the time between 1200 hours to 2000 hours LT the angle lay between 0° to 30°.

The records used in this analysis were not preselected except for a minimum level of activity as described in Chapter III. While nighttime records were considered to be predominantly of the Pi type and daytime records predominantly Pc, the results shown here indicate that no significant difference exists between these types of micropulsations as far as the parameters measured in this work are concerned. Indeed, spectral analysis could

not be expected to resolve these categories. Therefore, the averaged results presented in Chapter III are really the overall polarization characteristics of the micropulsation spectrum throughout the 24 hour day.

4.2 Suggestions for Further Research

Since polarization characteristics correlate well between simultaneous field and Observatory records, it would be useful to compare the same characteristics obtained from micropulsations recorded at conjugate point stations. Averaged results would perhaps clarify the mode of propagation of signal between the two hemispheres.

The data as it becomes available from the Observatory can be used to establish seasonal and yearly trends in the polarization characteristics.

Record sections longer than those used in this work will also allow the extension of this type of analysis to longer periods.

BIBLIOGRAPHY

Bendat, J.S. and A.G. Piersol, 1966. Measurement and analysis of random data, John Wiley and Sons, Inc., New York.

Blackman, R.B. and J.W. Tukey, 1958. The measurement of power, Dover Pulication, New York.

Born, M. and E. Wolf, 1959. Principles of Optics. Pergamon Press, New York.

Campbell, W.H., 1967. Geomagnetic pulsations. Physics of Geomagnetic Phenomena, Academic Press, New York, p. 821-909.

Campbell, W.H., 1966. A review of the equatorial studies of rapid fluctuations in the earth's magnetic field. Ann. Geophys., v. 22, p. 492-501.

Christoffel, D.A. and J.G. Linford, 1966. Diurnal properties of the horizontal geomagnetic micropulsation field in New Zealand. J. Geophys. Res., v. 71, p. 891-897.

Cooley, J.W. and J.W. Tukey, 1965. An algorithm for the machine calculations of complex Fourier series. Mathematics of Computation, v. 19, p. 297-307.

Fowler, R.A., B.J. Kotick and R.D. Elliott, 1967. Polarization analysis of natural and artificially induced geomagnetic micropulsations. J. Geophys. Res., v. 72, p. 2871-2883.

Gentleman, W.M. and G. Sande, 1966. Fast Fourier transform for fun and profit. AFIPS proc., Fall Joint Computer Conf., v. 29, p. 563-578.

Herron, T.J., 1967. An average geomagnetic power spectrum for the period range 4.5 to 12,900 seconds. J. Geophys. Res., v. 72, p. 759-761.

Hirasawa, T. and T. Nagata, 1966. Spectral analysis of geomagnetic pulsations from 0.5 to 100 seconds in period for the quiet sun condition. *Pure and Appli. Phys.*, v. 65, p. 102-124.

Jacobs, J.A., Y, Kato, S. Matsushita and V.A. Troitskaya, 1964. Classification of geomagnetic micropulsations. *J. Geophys. Res.*, v. 69, p. 180-181.

Jacobs, J.A. and K. Sinno, 1960a. World-wide characteristics of geomagnetic micropulsations. *Geophys. J.*, v. 3, p. 333-353.

Jacobs, J.A. and K. Sinno, 1960b. Occurrence frequency of geomagnetic micropulsations Pc. *J. Geophys. Res.*, v. 65, p. 107-113.

Jacobs, J.A., K.O. Westphal, 1964. Geomagnetic micropulsations. *Physics and Chemistry of the Earth*, v. 5, Pergamon Press, New York, p. 157-224.

Kato, Y., 1964. Regular oscillations with periods of 5 seconds to 7 minutes. *N.B.S. Rept. 8815, Symposium on Ultra Low Frequency Electromagnetic Fields, Boulder, Colorado*.

Kato, Y., J. Ossaka, T. Watanabe, M. Okuda and T. Tamao, 1956. Investigation on the magnetic disturbance by the induction magnetograph, part V on the rapid pulsation, p.s.c. *Sci. Rept. Tôhoku Univ. 5, Geophys.*, v. 7, p. 136-146.

Kato, Y. and T. Saito, 1959. Preliminary studies on the daily behavior of rapid pulsation. *J. Geomagn. Geoelect.*, v. 10, p. 221-225.

Kato, Y. and T. Utsumi, 1964. Polarization of long period geomagnetic pulsation, Pc5. *Sci. Rept. Tôhoku Univ. 5, Geophys.*, v. 15, p. 83-96.

Kawamura, M., K. Kurusu, H. Oshima and K. Yanagihara, 1961. On the geomagnetic pulsation pc-(I), world-wide distribution of the horizontal disturbing vector. Mem. Kakioka Magn. Obs. Suppl., v. 10, p. 7-13.

Mather, K.B., K.J. Gauss and C.R. Cresswell, 1964. Diurnal variations in the power spectrum and polarization of telluric currents at conjugate points, L = 2.6. Australian J. Phys., v. 17, p. 373-388.

Nwaigwe, C.N.C., S.H. Hall, and M.J. Usher, 1967. Systematic diurnal variations in the period and polarization of magnetic micropulsations in south-west England. Nature, v. 214, p. 1319-1321.

Parzen, E., 1961. Mathematical considerations in the estimation of spectra. Technometrics, v. 3, p. 167-189.

Paulson, K.V., 1968. The polarization and spectral characteristics of some high-latitude irregular micropulsations. Ann. Geophys., v. 24, p. 261-266.

Paulson, K.V., A. Egeland and F. Eleman, 1965. A statistical method for quantitative analysis of geomagnetic giant pulsations. J. Atmosph. Terr. Phys., v. 27, p. 943-967.

Rankin, D. and I.K. Reddy, 1969. A magnetotelluric study of resistivity anisotropy. Geophysics, v. 34, p. 438-449.

Romañá, A. and J.O. Cardús, 1962. Geomagnetic rapid variations during I.G.Y. and I.G.C.. J. Phys. Soc. Japan, v. 17, Supp. A-II, p. 47-55.

Rostoker, G., 1967a. The frequency spectrum of Pi2 micropulsation activity and its relationship to planetary magnetic activity. J. Geophys. Res., v. 72, p. 2032-2039.

Rostoker, G., 1967b. The polarization characteristics of Pi2 micropulsations and their relation to the determination of possible source mechanisms for the production of nighttime impulsive micropulsation activity. Can. J. Phys., v. 45, p. 1319-1335.

Saito, T., 1969. Geomagnetic pulsations. In press.

Saito, T., 1964. Mechanisms of geomagnetic continuous pulsations and physical states of the exosphere. J. Geomagn. Geoelec., v. 16, p. 115-151.

Saito, T. and S. Matsushita, 1968. Solar cycle effects on geomagnetic Pi2 pulsations. J. Geophys. Res., v. 73, p. 267-286.

Sano, Y., 1963. Morphological studies on sudden commencements of magnetic storms using rapid-run magnetograms (including studies on sudden impulses), (II). Mem. Kakioka Mag. Obs., v. 11, p. 1-52.

Voelker, H., 1968. Observations of geomagnetic pulsations: Pc3, 4 and Pi2 at different latitudes. Ann. Geophys., v. 24, p. 245-252.

Yanagihara, K., 1959. Some characters of geomagnetic pulsation Pt and accompanied oscillation SPt. J. Geomag. Geoele., v. 10, p. 172-176.

Zybin, K. Yu, 1967. On the polarization characteristics of middle latitude geomagnetic micropulsations. Indian J. of Met. and Geophys., v. 18, p. 349-354.

Zybin, K. Yu, 1965. Properties and nature of geomagnetic micropulsations with periods from 10 seconds to several minutes. Geomagn. Aeronomy, v. 5, p. 380-383.